

Spring 5-31-2008

Design and construction of a novel transpalpebral ophthalmic tonometer

Philippe R. Moinot
New Jersey Institute of Technology

Follow this and additional works at: <https://digitalcommons.njit.edu/theses>



Part of the [Biomedical Engineering and Bioengineering Commons](#)

Recommended Citation

Moinot, Philippe R., "Design and construction of a novel transpalpebral ophthalmic tonometer" (2008).
Theses. 366.
<https://digitalcommons.njit.edu/theses/366>

This Thesis is brought to you for free and open access by the Electronic Theses and Dissertations at Digital Commons @ NJIT. It has been accepted for inclusion in Theses by an authorized administrator of Digital Commons @ NJIT. For more information, please contact digitalcommons@njit.edu.

Copyright Warning & Restrictions

The copyright law of the United States (Title 17, United States Code) governs the making of photocopies or other reproductions of copyrighted material.

Under certain conditions specified in the law, libraries and archives are authorized to furnish a photocopy or other reproduction. One of these specified conditions is that the photocopy or reproduction is not to be “used for any purpose other than private study, scholarship, or research.” If a user makes a request for, or later uses, a photocopy or reproduction for purposes in excess of “fair use” that user may be liable for copyright infringement,

This institution reserves the right to refuse to accept a copying order if, in its judgment, fulfillment of the order would involve violation of copyright law.

Please Note: The author retains the copyright while the New Jersey Institute of Technology reserves the right to distribute this thesis or dissertation

Printing note: If you do not wish to print this page, then select “Pages from: first page # to: last page #” on the print dialog screen

The Van Houten library has removed some of the personal information and all signatures from the approval page and biographical sketches of theses and dissertations in order to protect the identity of NJIT graduates and faculty.

ABSTRACT

DESIGN AND CONSTRUCTION OF A NOVEL TRANSPALPEBRAL OPHTHALMIC TONOMETER

by

Philippe R. Moinot

Glaucoma –a degeneration of the optic nerve- is a leading cause of blindness which is primarily caused by large fluctuations in intraocular pressure (IOP) known as diurnal variations. Because these peak in the early morning dropping off rapidly, a self administrable and inexpensive IOP home testing procedure is highly desirable. The approach contained herein –unlike traditional Goldman applanation tonometry which requires the use of ophthalmic anesthetics and complex diagnostic equipment- describes a novel IOP measurement method consisting of concavation of the cornea or sclera through the palpebra superior by the spherical tip of an optoelectronic photodetector suspended in a force sensing probe. Three subjects participated in an experiment in which a prototype device was tested alongside traditional measurement techniques in a clinical setting. Whilst the device was designed to be initially calibrated to each individual subject for palpebral color, reflectivity and thickness, uncompensated preliminary data collected disclose proof of concept.

**DESIGN AND CONSTRUCTION OF A NOVEL
TRANSPALPEBRAL OPHTHALMIC TONOMETER**

by
Philippe R. Moinot

**A Thesis
Submitted to the Faculty of
New Jersey Institute of Technology
in Partial Fulfillment of the Requirements for the Degree of
Master of Science in Biomedical Engineering**

Department of Biomedical Engineering

May 2008

Blank Page

APPROVAL PAGE

**DESIGN AND CONSTRUCTION OF A NOVEL
TRANSPALPEBRAL OPHTHALMIC TONOMETER**

Philippe R. Moinot

Dr. Tara Alvarez *o* Date
Associate Professor of Biomedical Engineering, NJIT

Dr. Max Roman Date
Biomedical Engineering Masters Program Director, NJIT

Dr. Mesut Sahin Date
Assistant Professor of Biomedical Engineering, NJIT

BIOGRAPHICAL SKETCH

Author: Philippe R. Moinot

Degree: Master of Science

Date: May 2008

Undergraduate Education:

- Master of Science in Biomedical Engineering
New Jersey Institute of Technology, Newark, NJ, 2008
- Bachelor of Science in Biomedical Engineering
New Jersey Institute of Technology, Newark, NJ, 2005
- Bachelor of Science in Electrical Engineering Technology
New Jersey Institute of Technology, Newark, NJ, 1998
- Associate of Applied Science in Electrical Engineering Technology
Hudson County Community College, Jersey City, NJ, 1989

Major: Biomedical Engineering

Presentations and Publications:

- P. R. Moinot and T. L. Alvarez, Ph. D., "*Design and Construction of a Novel Transpalpebral Ophthalmic Tonometer*," in 34th Annual Northeast Bioengineering Conference (NEBC), Princeton, RI, 2008.
- P. R. Moinot, L. Simone, Ph. D., and S. Reisman, Ph. D., "*A Four Quadrant Inertial Mass Torque Reactor Based Road Vibration Source For Spatial Enhancement Of Virtual Reality Driving Simulators*," in IEEE 31st Annual Northeast Bioengineering Conference (NEBC), Hoboken, NJ, 2005.
- P. R. Moinot, "*Design, Construction and Programming of a Personal Computer Based Scanning Acoustic Microscope for Orthopædics Research*," in NJIT Biomedical Engineering Society (BMES) Proceedings, Newark, NJ, 2005.

To my beloved parents Michel and Jacqueline Moinot

ACKNOWLEDGEMENT

I would like to express my deepest appreciation to Dr. Tara Alvarez for her tireless efforts both as my thesis advisor and in her immeasurable research inspiration, support and insight. Special thanks are given to Dr. Max Roman and Dr. Mesut Sahin for actively participating in my committee.

I wish to thank the Biomedical Engineering Department and the National Science Foundation for their financial consideration as well as N&J Machine Products of Newark, NJ for their generous technical support and unlimited use of their machine shop facilities.

Finally, I'd like to thank Michele A. Kessler for her angelic patience as I completed this research.

TABLE OF CONTENTS

Chapter	Page
1 INTRODUCTION	1
1.1 Objectives	1
1.2 Background	1
1.2.1 Glaucoma Mechanism and Statistics.....	1
1.2.2 Glaucoma Factors	6
1.2.3 Traditional Diagnostic Techniques	6
2 HOME BASED IOP TESTING	11
2.1 Problem Statement	11
2.2 Design Solution Parameters	11
2.2.1 Cost	11
2.2.2 Ease of Use	12
2.2.3 Comfort	12
3 IMPLEMENTATION	13
3.1 Operating Principle	13
3.2 Scope of Prototyping	14
3.2.1 Concept Limitation	14
3.2.2 IRB Limitations	14
3.2.3 Clinical Limitations	14
3.2.4 Resulting Scope	15

TABLE OF CONTENTS
(Continued)

Chapter	Page
3 IMPLEMENTATION (Continued)	
3.3 Prototype Design and Construction	15
3.3.1 Photodetecting Probe Tip	15
3.3.2 Force Sensing Mechanism	16
3.3.3 Suspension mechanism	19
3.3.4 Illuminator	21
3.3.5 Signal Conditioning	23
3.3.6 Sensing Head Assembly	26
3.3.7 Data Acquisition System	27
4 RESULTS	30
4.1 Clinical Trials	30
4.1.1 Goldman Applanation Tonometry	30
4.1.2 Prototype Device Sampling	30
5 CONCLUSION	42
5.1 Comparison	42
5.2 Future Work	43
5.2.1 Illuminator Design	43
5.2.2 Linear Guide Mechanism	43
5.2.3 Intuitive Azimuthal Orientation	43
APPENDIX LABVIEW DAQ VI BLOCK DIAGRAMS	44
REFERENCES	49

LIST OF FIGURES

Figure	Page
1.1 Blood supply to the eye.....	2
1.2 Gross anatomy and schematic depiction of the retina	3
1.3 Normal and impaired aqueous flow	4
1.4 Goldman applanation tonometer	7
3.1 Operating principle schematic	13
3.2 Photodetecting probe tip	15
3.3 LVDT and spring assembly	17
3.4 Subminiature full bridge strain gage based shear beam load cell	18
3.5 Load cell operating principle	18
3.6 Lever arm suspension mechanism	20
3.7 Dual recirculating linear ball slide	21
3.8 Lightpipe illuminator	22
3.9 Infrared thermograph of illumination field around probe tip	22
3.10 IRLED illuminator circuitry	23
3.11 Photodetector circuitry	24
3.12 Load cell signal conditioning circuitry	25
3.13 Signal conditioning circuitry	26
3.14 Sensing head	26
3.15 Power conditioning circuitry	27
3.16 Complete system	28
3.17 Virtual instruments	29

LIST OF FIGURES
(Continued)

Figure	Page
4.1 Stereoscopic images of three typical time sample series	32
4.2 Scatter plot	33
4.3 6th order polynomial fit	34
4.4 Linear fit	34
4.5 Subject #1 pre-supine average compliances	35
4.6 Subject #2 pre-supine average compliances	36
4.7 Subject #3 pre-supine average compliances	37
4.8 Subject #1 post-supine average compliances	39
4.9 Subject #2 post-supine average compliances	40
4.10 Subject #3 post-supine average compliances	41
5.1 Correlation coefficient	42
A.1 Labview VIs block diagram overview.....	44
A.2 Acquisition initialization VI	45
A.3 Board enumeration	45
A.4 Channel and trigger enumeration	46
A.5 Trigger parameters.....	46
A.6 Scans	47
A.7 While loop	48

LIST OF TABLES

Table	Page
4.1 Experimental results	38

CHAPTER 1

INTRODUCTION

1.1 Objectives

The objective of this thesis is to present the chronology of a novel design and construction proof of concept research project pertaining to a biomedical diagnostic instrument -and its associated operational protocol- destined for use in the treatment of glaucoma.

This instrument –a transpalpebral ophthalmic tonometer- is intended –as its name suggests- to measure a subject’s intraocular pressure (IOP) through the *palpebra superior* (or upper eyelid). This has come to be accomplished using the combination of an infrared illuminator array, a hemispherical photodetecting probe tip and a full bridge strain gage based load cell with their associated signal conditioning circuits and computational system.

1.2 Background

The following subsections describe the *raison d’être* for this research project.

1.2.1 Glaucoma Mechanism and Statistics

One leading cause of blindness is glaucoma, which is defined as damage to the optic nerve resulting in visual field loss. Glaucoma is believed to be most often caused by elevated IOPs constricting the retinal arteries and veins (Figure 1.1) which lead to and from retinal ganglion cells (Figure 1.2) which collectively transmit visual information from the retina to several regions in the thalamus, hypothalamus, and mesencephalon.

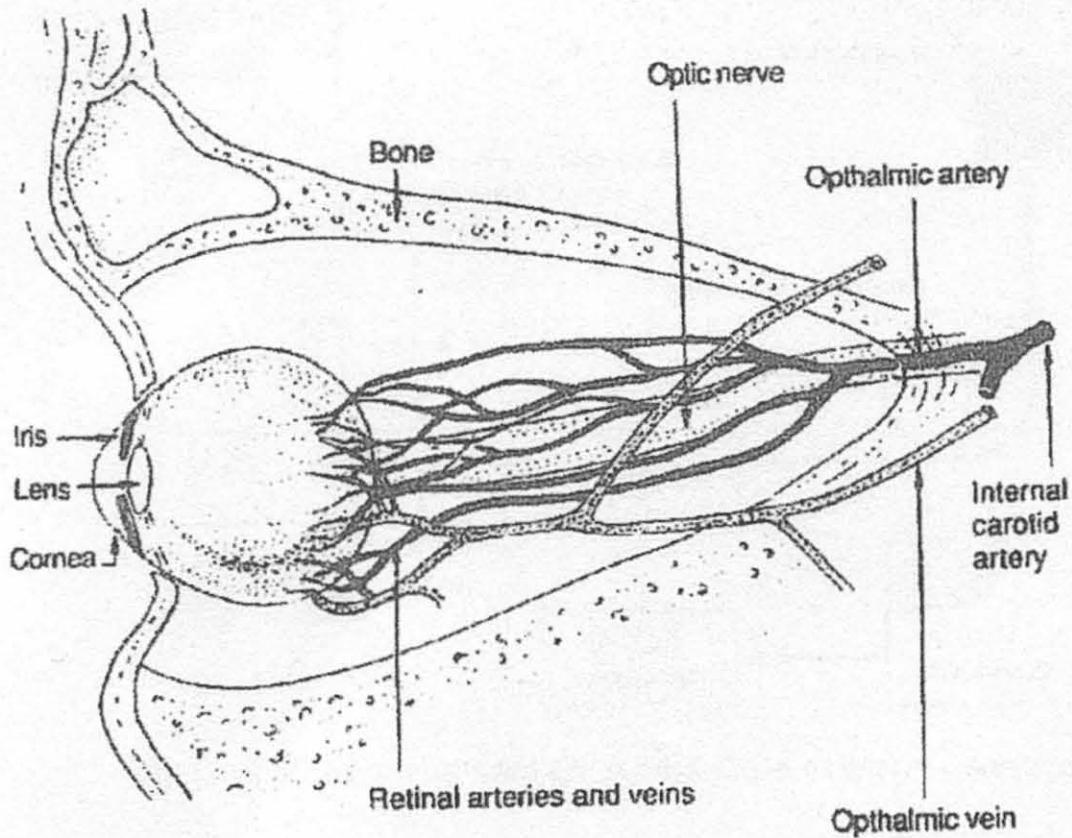
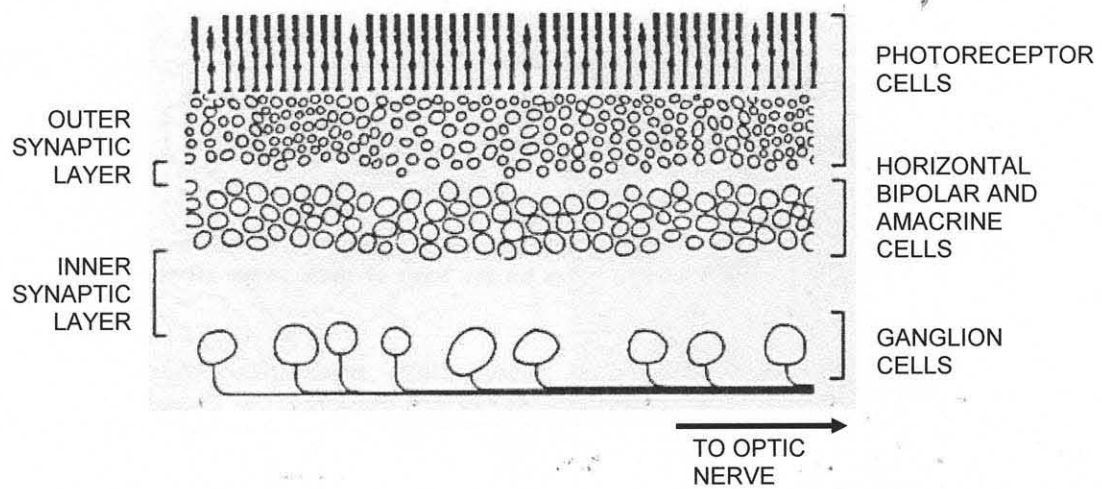
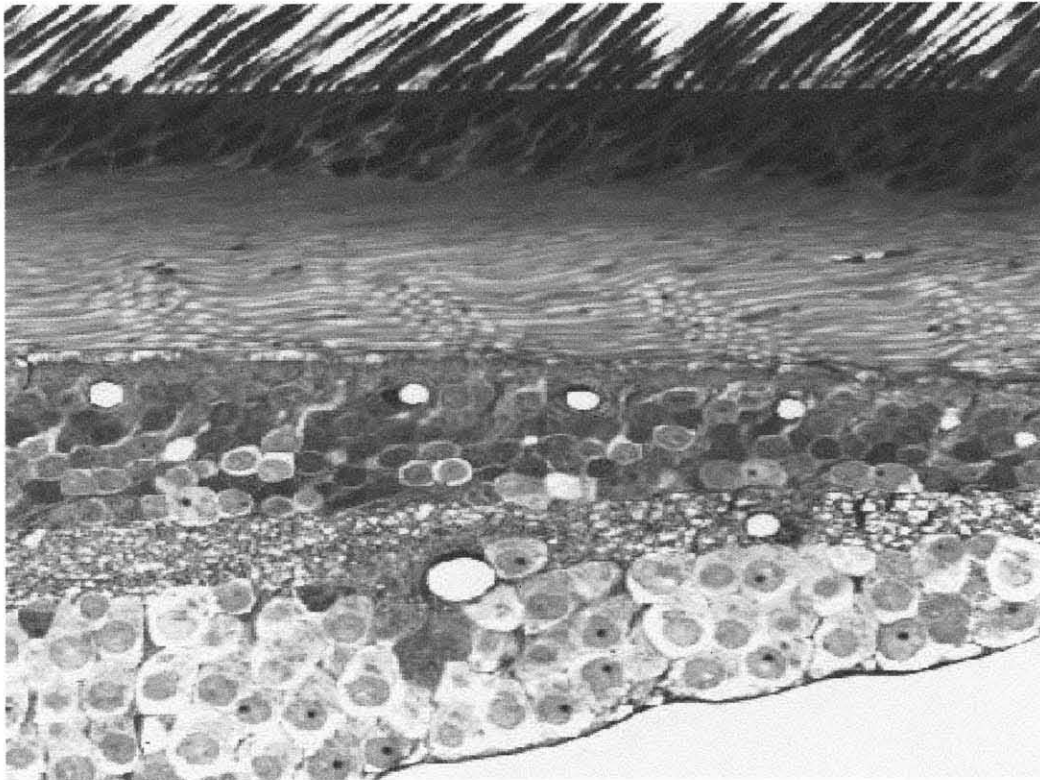


Figure 1.1 Blood supply to and from the eye [7].

Glaucoma cases fall into one of three major categories. These are: primary open angle glaucoma –in which Schlemm’s canal is subject to blockages,- angle closure –in which the aqueous humor is prevented from draining around the iris.- (both in Figure 1.3) and non-IOP related. The latter category –most often found in subjects of Asian and Arctic descent- does not lend itself to use of the novel device described herein as the device’s operation uniquely concerns IOP measurement.

Eye disorders and blindness are estimated to cost the nation more than \$16 billion annually. [8] Even with proper treatment, 10% of patients afflicted with optic nerve degeneration experience loss of vision.

FRONT



REAR

Figure 1.2 Gross anatomy [4] (top) and schematic depiction [5] (bottom) of the retina in transverse section view.

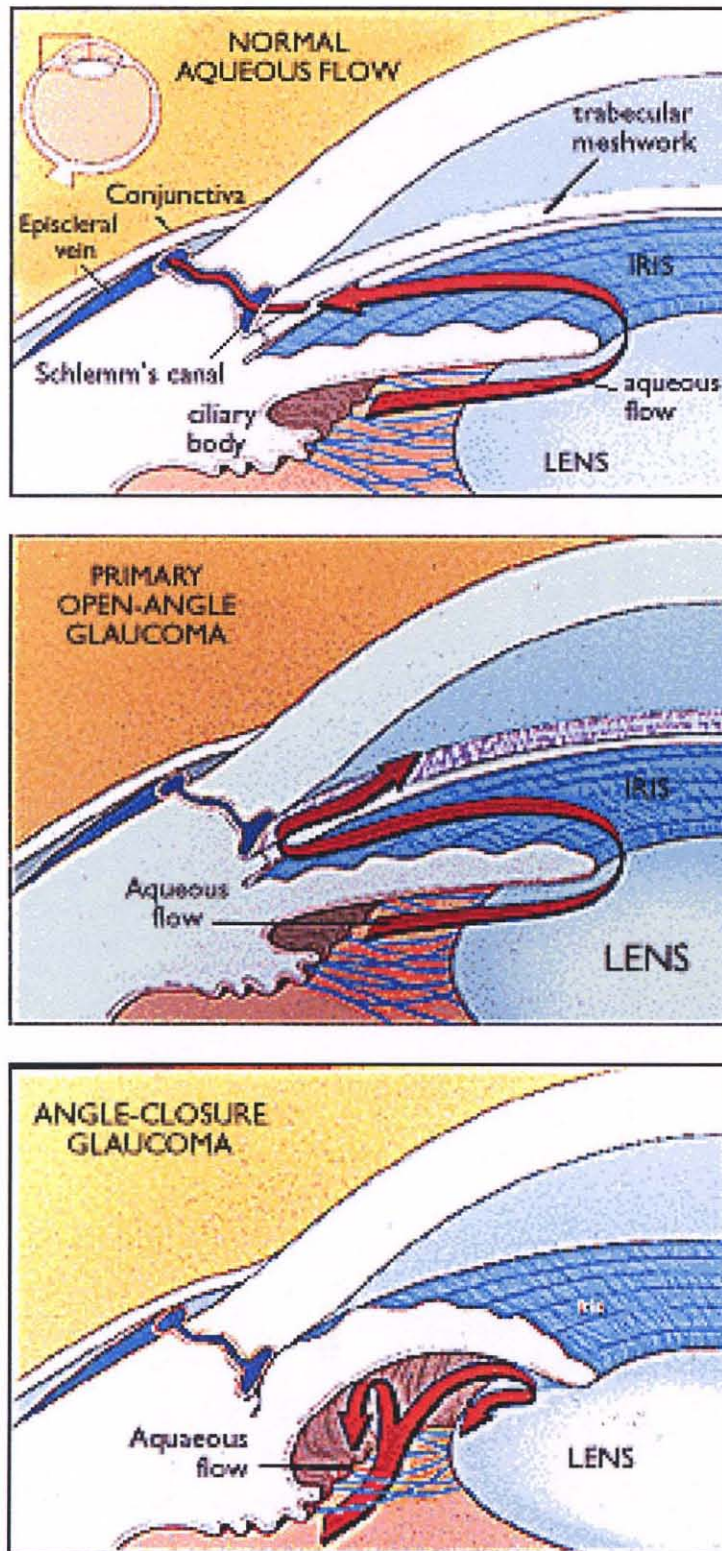


Figure 1.3 Normal and impaired aqueous flow [6].

Prevent Blindness America estimates that over 3 Million Americans have glaucoma but only half of those know that they have it. The National Eye Health Program of the National Institutes of Health approximates that 120,000 are blind from glaucoma, accounting for 9% to 12% of all cases of blindness in the U.S., that glaucoma is the leading cause of blindness among African-Americans and that two million Americans currently have glaucoma. [8] Other studies estimate that due to the aging population this number will increase to 3.3 million by 2020. [9]. The World Health Organization lists glaucoma as the second leading cause of blindness in the world. Estimates put the total number of suspected cases of glaucoma at around 65 million worldwide.

The critical measurement attained in the management of a patient's vision with glaucoma is intraocular pressure (IOP) using a tonometer. Researchers have shown that IOP varies throughout the day [1] and glaucoma patients only have their IOP measured every few months. [10] Other health sectors have home monitoring devices that are critical in the management of disease such as glucometers which measure glucose levels for diabetics and blood pressure monitors both of which are routinely used in the home. Analogously, if an ophthalmologist could instruct his patients to monitor IOP periodically throughout the day, the management of the patient's vision with glaucoma would be dramatically improved by slowing their resistance to IOP lowering medications. Our research team is actively involved in research, development and validation of point-of-care tonometer devices.

1.2.2 Glaucoma Factors

There is no cure for glaucoma. As a chronic condition, life long monitoring of intraocular pressure (IOP) is required. With proper IOP monitoring and corresponding administration of medication, further degeneration can be halted. It was long thought that static elevated IOPs were the main cause of glaucoma. Recent studies have revealed that elevated changes in pressure known as diurnal variations are of primary concern in the progression of blindness in glaucoma patients [1]. Furthermore, studies indicate that IOP is actually at its highest first thing in the morning before a patient can go to their physician's office [2]. For this reason, an inexpensive home based measurement technique is highly desirable.

1.2.3 Traditional Diagnostic Techniques

The gold standard for ophthalmic tonometry has long been Goldman applanation tonometry. This procedure –routinely performed in common eye examinations- involves the applanation (or flattening) of the *cornea* (or lens) –using the combination of a truncated conic optic element and a slit lamp projector (Figure 1.4)- subsequent to the application of a topical ophthalmic anesthetic. The applied force required to produce a given amount of applanation correlates quite well to the intraocular pressure. Though not terribly invasive, this procedure does require anesthetics and bulky, high precision and expensive diagnostic equipment and must be administered by a trained physician or clinician.



Figure 1.4 Goldman applanation tonometer (left), applanation optic and slit lamp (middle) and mires (right) which indicate degree of applanation.

The eyeball surface is composed of the sclera (white of the eye) and cornea (transparent tissue distal to the lens). The Imbert-Fick Law shows that when approximating the eyeball as a sphere, the IOP will be equal to the applied force divided by the contact area of a fully applanating tip pressed upon the cornea. Mackay and Marg showed that IOP can be determined in this way with the use of an excursion limiting ring coaxial to the corneal applanation tip. Where sufficient force is applied directly to the cornea for applanation to occur beyond the inner diameter of the ring, an inflection point in the force versus time curve is created. At this point the IOP is equal to the force applied divided by the tip area. [11]

Our tonometer design operates in much the same manner, but using a hemispherical –rather than flat- tip applied to the cornea through the eyelid eliminating the need for anesthetics. Furthermore, rather than relying on a skilled clinician to provide a time-linear application of force, we introduce a second sensor –in addition to the force sensor- which optoelectronically measures obscuration (tip penetration) eliminating dependence on the time variable. Unlike Mackay Marg's, which was intended for the clinic, our tonometer will be used by the patient at home.

Intraocular pressure (IOP) is monitored in glaucoma patients with measurement intervals ranging from days to months rather than hours. [10] Tonometry performed during routine glaucoma examinations thus only provides the physician with a glimpse of intraocular pressure. Asrani and colleagues showed that although patients had similar average and standard deviation for home and office IOP, large fluctuations in diurnal IOP were still a significant risk for glaucoma progression. [1] The magnitude of the variations in IOP is also potentially an important clinical indicator since it is correlated with loss of visual field. [1] Zeimer and colleagues concluded that peaks in IOP tend to occur in the early morning, typically right after waking before a patient can reach the clinic, and may have an effect on loss of vision. [2] There is therefore a clinical need for an effective point-of-care tonometry method, particularly one that would allow a patient to measure his IOP between visits to decrease vision loss associated with glaucoma.

Typical clinical tonometers, such as the Goldman tonometer, utilize direct corneal applanation, which requires anesthetizing the eye. Although these instruments are accurate and precise, they are not practical for home monitoring, as many patients would have difficulty applanating their own cornea, and there is no approved topical anesthetic for home use. One “home” tonometer developed by Zeimer and colleagues requires a topical anesthetic or the use of a contact lens. [13] A preferable tonometer would not require anesthetic and would be simple to use, sufficiently accurate and most of all inexpensive.

Fresco and Dayman have invented a method and a device based on the principle that pressure applied to the sclera generates a phosphene spot, a self-perceptible visual phenomenon. [14] The Proview™ Eye Pressure Monitor is a phosphene tonometer

approved by the FDA and recently marketed by Bausch & Lomb. Our team's -including Alvarez and colleagues [3]- clinical evaluation compared the Proview™ with the Goldmann tonometer and yielded a correlation coefficient of $r=0.41$. The sensitivity of the Proview™ technique to detect patients with high IOP was low, since the value of the Proview™ pressure only identified 18% (4/22) of these patients. In other words, the Proview™ failed to detect high pressure in 4 out of 5 patients with glaucoma, the key market application for this device. Clearly, this tonometer does not meet its market requirements. This further indicates the need for a home use tonometer for the management of a glaucoma patient's vision.

Increased IOP is an indicator of glaucoma. Several researchers state the need for patients to be able to measure their IOP regularly at home. [1][12][13][14] Many home tonometers on the market are not reliable. [3][12] Those on the market in Europe and proposed elsewhere require an anesthetic because the devices are painful and thus unsuitable for home use in the US. [15] In this project, we developed, clinically evaluated, and improved a tonometer for patients with glaucoma. Our team has evaluated the Proview™ and published in the peer reviewed journal Ophthalmology our findings that this FDA approved tonometer marketed by Bausch & Lomb only detects high pressure in 1 out of 5 patients who have glaucoma. This device clearly does not meet the clinical need. We have developed a proprietary concept through IRB approved clinical studies, including preliminary data that suggest clinical potential. We have used the same methodology to correlate performance of our tonometer against the clinical gold standard Goldman tonometer using the protocol developed by Dr. Fechtner for our evaluation of the Proview™ product. Given successful development and validation, the NJIT

tonometer shall provide precise and accurate IOP measurement for glaucoma patients in the convenience of their own homes decreasing the amount of visual field loss and enabling timely and accurate determination of the timing and dose of drug required to optimally maintain normal physiological levels of IOP.

Other IOP measurement approaches have been successfully realized, but they all lack in self-administrable ease of use and / or are exceedingly expensive. Previous attempts at home based, inexpensive and self-administered IOP tests have proven ineffective [3].

CHAPTER 2

HOME BASED IOP TESTING

2.1 Problem Statement

What is required for the proper care of glaucoma patients is a personal IOP measurement diagnostic device which may be used upon waking –when IOPs are known to peak- in order to properly regulate the administration of their IOP stabilizing medications. When compared to currently available methods, this device and its associated operational protocol should be relatively inexpensive and easily self administrable, comfortable and completely non-invasive. It should be small, lightweight, power thrifty and require little to no maintenance.

2.2 Design Solution Parameters

The following subsections enumerate and describe the design constraints implemented to address the problems listed in the latter section.

2.2.1 Cost

In order to make the device available to all glaucoma patients, it must be designed for a manufacturing cost of approximately twenty dollars enabling a retail cost to the patient of less than one hundred dollars plus the expense of a one time clinical visit for initial calibration. This excludes the use of exotic materials and components, as well as time or expensables intensive manufacturing techniques.

2.2.2 Ease of Use

The device should require little training and no special skills to use. The design should lend itself to a device that is small enough to easily tuck into a pocket and comprise its own low maintenance power source such as lithium coin cells. It should also be easy to clean and fairly resistant to environmental contamination.

2.2.3 Comfort

To encourage regular use of the device, it should cause the patient to experience little to no discomfort without the use of anesthetics. This precludes any direct contact with the surface of the eye.

CHAPTER 3

IMPLEMENTATION

3.1 Operating Principle

The current device has gone through several iterations which will be described in detail below. The following refers to Figure 3.1 which schematically depicts the device's operating principle and components.

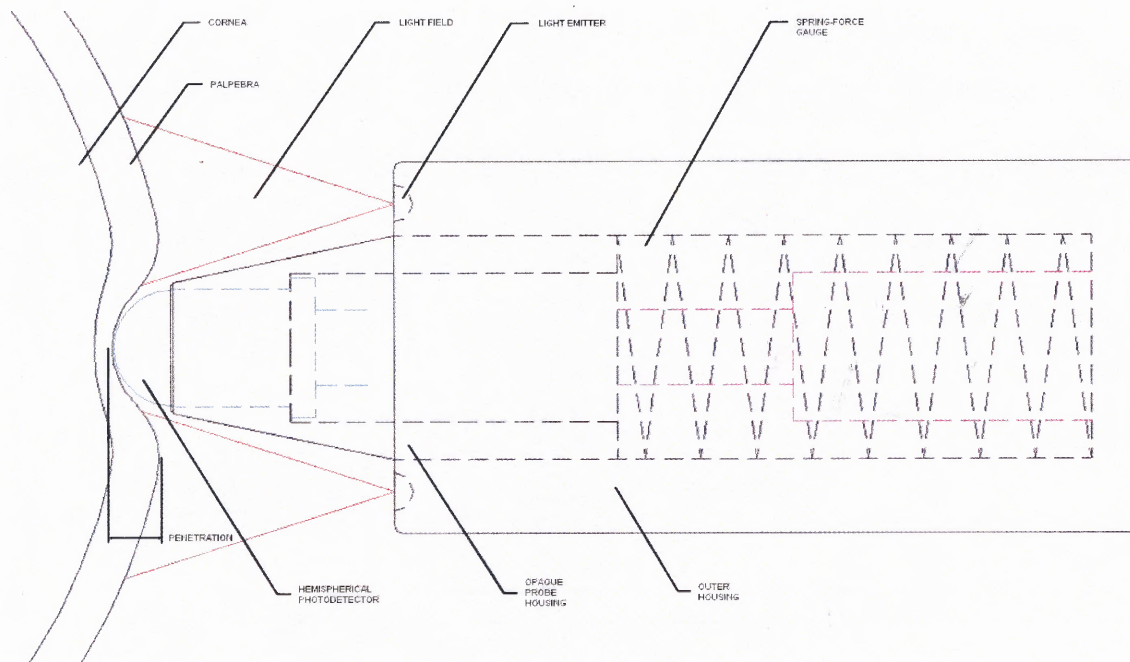


Figure 3.1 Operating principle schematic.

A hemispherically tipped infrared photodiode (cyan) housed in a tapered cylinder is manually pressed upon the *palpebra superior* via a spring loaded outer housing. The outer housing incorporates a displacement sensor (magenta) as well as an illuminator ring (rays in red). As the probe is pressed onto the eye with increasing force, the

photodetector is gradually obscured yielding a measure of penetration. IOP can then be extrapolated as a function of probe tip penetration with respect to the applied force which is measured by the spring and displacement sensor combination.

3.2 Scope of Prototyping

This section describes the purpose -or expected benefits- for the form of this prototype device's design and construction.

3.2.1 Concept Limitation

The variability of palpebral geometry and coloration –most notably its thickness, elasticity and reflectivity at the illuminator's wavelength- necessitate calibration of the device –at least computationally- to each subject. Due to the aforementioned limitation, verifying operational details such as gain and linearity would require standards comparison testing at a minimum of two and three significantly different IOPs per subject respectively.

3.2.2 IRB Limitations

At the current stage of concept development, obtaining IRB approval for altering an approved test subject's IOP through the administration or suspension of medications is not justified limiting our ability to fully evaluate the aforementioned operational details.

3.2.3 Clinical Limitations

It was hoped that side by side comparison testing between Goldman applanation tonometry and the prototype device would yield appreciable correlation data within each subject when performed in a standing position both pre and post a ten minute supination

period. [14] [16] However, the supination period failed to significantly affect the IOP as measured in the Goldman reference tests.

3.2.4 Resulting Scope

For these reasons, in anticipation of broadening IRB approval, prototype construction and testing were limited to proving that the mechanism's design would exhibit a specific relationship in terms of penetration with respect to applied force. That relationship being that the palpebral compressible region does not intersect that of the cornea or sclera. In other words, that the penetration with respect to applied force function would indicate – within a range of applied force- separate compressible regions for the palpebra and cornea or sclera such that the palpebral compressibility might be disregarded.

3.3 Prototype Design and Construction

Several years of design and experimentation have led to the creation of the current prototype. This section depicts a synopsis of the design cycle.

3.3.1 Photodetecting Probe Tip

As the basis for the operating concept, the design of the probe tip (Figure 3.2) has

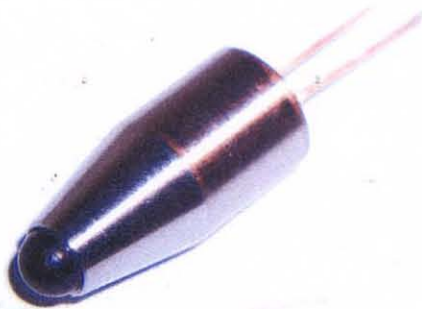


Figure 3.2 Stainless steel probe housing showing maximum protrusion setting of hemispherical photodetecting probe tip (calibration shims were uninstalled.)

changed little since the project's inception. The probe tip consists of a standard T1-3/4 rimmed hemispherically tipped infrared photodiode housed in a tapered 316 stainless steel cylinder. The photodiode's protrusion distance is controlled by the thickness of a replaceable spacing washer placed between the face of a step in the cylinder's bore and the photodiode's rim. The photodiode and spacer are held in place from behind by a bored and slotted nylon 6/6 (nonconductive) setscrew through which the photodiode's two conductors are passed.

3.3.2 Force Sensing Mechanism

The original design for the force sensing mechanism involved the creation of a custom linearly variable differential transformer (LVDT) and spring assembly (Figure 3.3). This design showed some promise but was abandoned due to tradeoffs in lateral rigidity versus friction factors. All subsequent designs incorporated a subminiature full bridge strain gage based shear beam load cell (Figure 3.4). This type of load cell's operating principle –as depicted in Figure 3.5- involves four strain gages operating in opposing pairs to form the legs of a full bridge. In order to operate properly, the reactive torques generated by the beam must be constrained to maintain parallelism in the beam ends. This maintains one pair of strain gages in tension and one pair in compression.

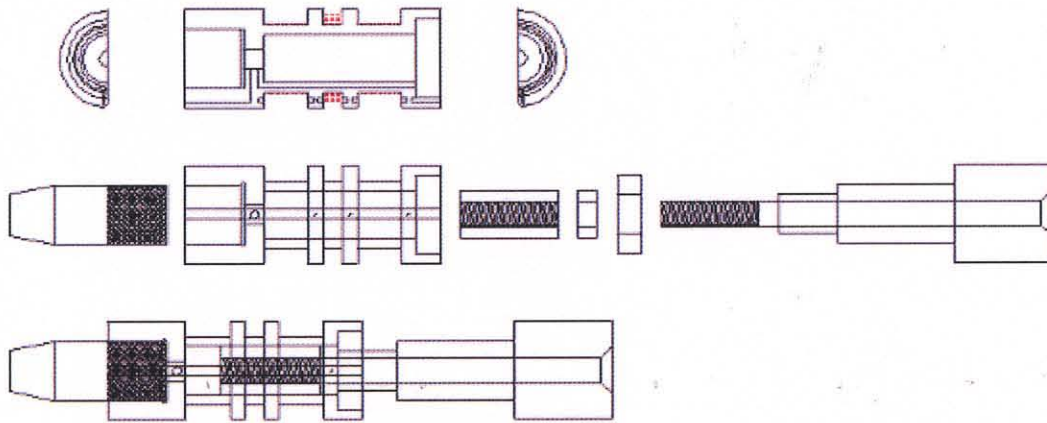
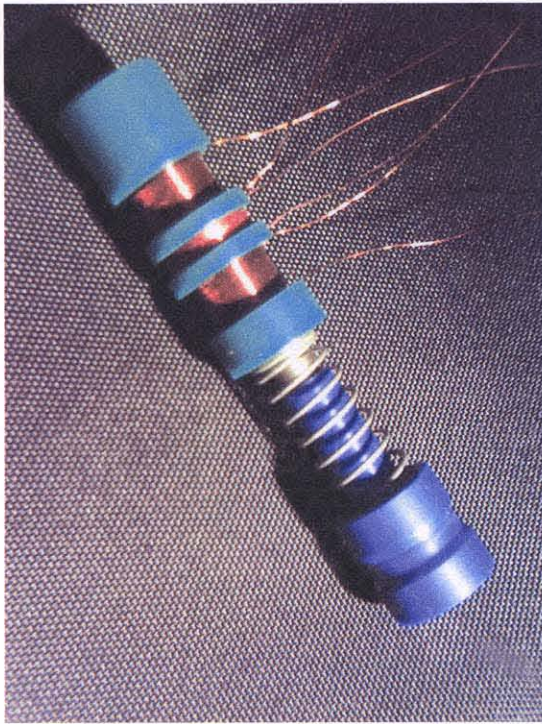


Figure 3.3 Abandoned LVDT and spring assembly.

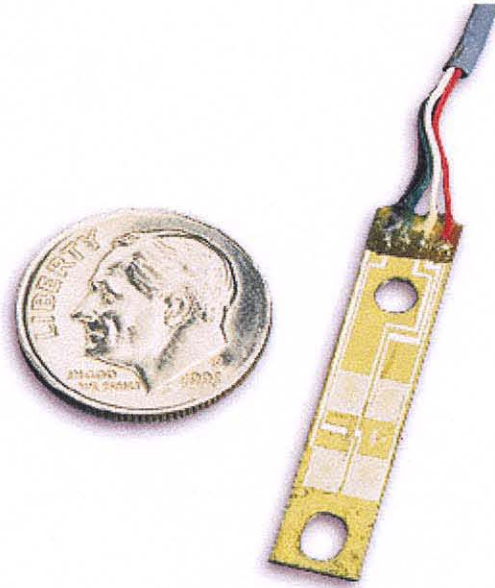


Figure 3.4 Subminiature full bridge strain gage based shear beam load cell.

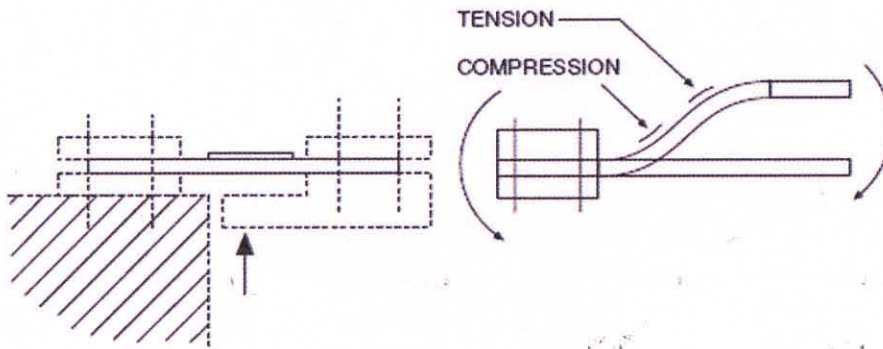


Figure 3.5 Load cell geometry.

3.3.3 Suspension Mechanism

The incorporation of several different probe tip and load cell suspension and constraint mechanisms was attempted.

The first attempt simply involved the use of a stainless steel block and brass bushing arrangement. This arrangement revealed drawbacks similar in nature to the LVDT force sensing arrangement.

The next mechanism (Figures 3.6) –in an effort to reduce friction and increase lateral constraint- incorporated a lever arm suspended by two axially aligned bearings. This arrangement showed great improvement but there still existed significant sensitivity to the application of lateral forces.

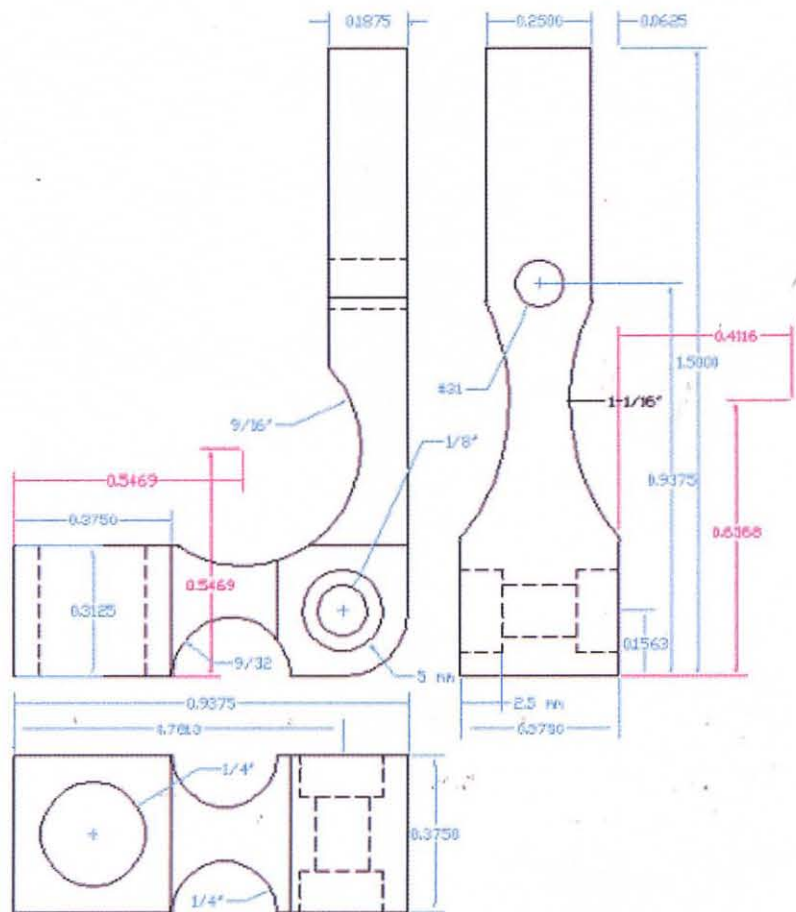
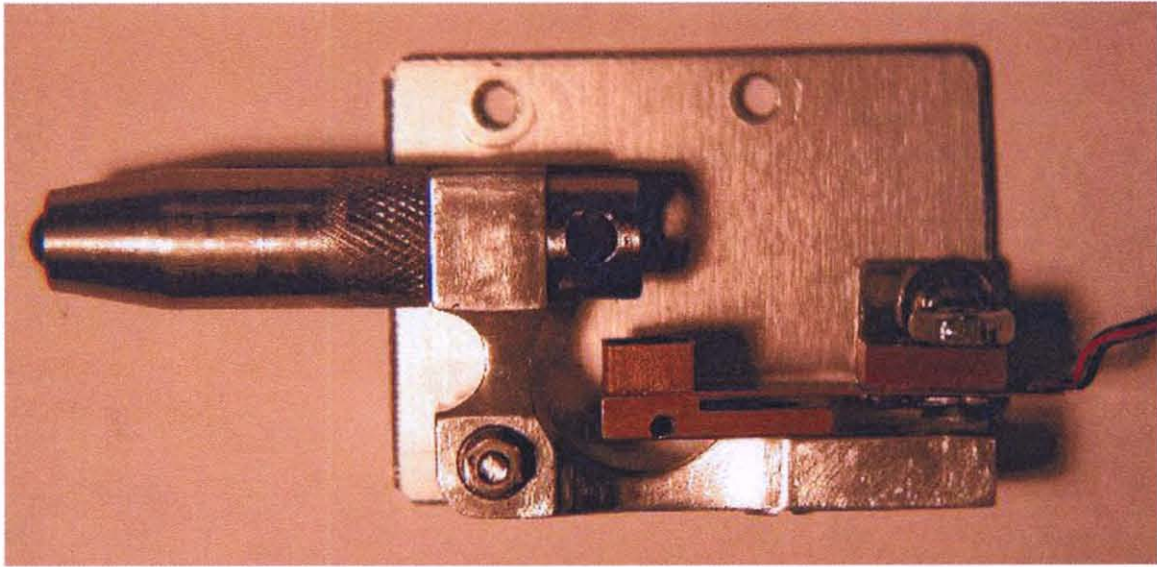


Figure 3.6 Abandoned lever arm suspension mechanism.

This was all but completely ameliorated in the most recent redesign which incorporates one of the world's smallest dual recirculating linear ball slide mechanisms (Figure 3.7).

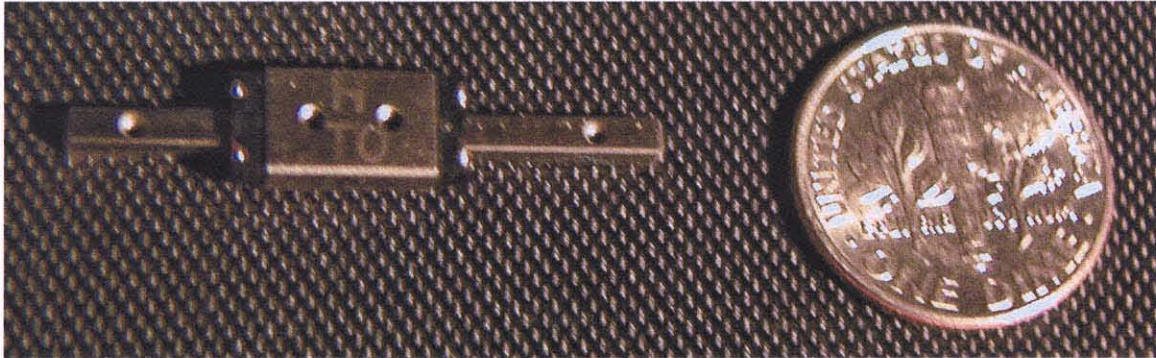


Figure 3.7 Dual recirculating linear ball slide.

3.3.4 Illuminator

The original illuminator concept (Figure 3.8) comprised a brass bushed backlit polymethylmethacrylate lightpipe. In order to facilitate testing of the device's other subassemblies –namely the force sensing components,- this idea was set aside in favor of a more accessible and manipulable –though admittedly less streamlined- direct projection system.



Figure 3.8 Lightpipe illuminator.



Figure 3.9 Infrared thermograph of uniform illumination field around probe tip (imaged using a chilled CCD detector to minimize thermal noise.)

Several light emitting diode (LED) sources of varying wavelength and dispersion angle and various mounting positions were tested until an acceptable –uniform and continuous- illumination field (Figure 3.9) was developed.

3.3.5 Signal Conditioning

The signal conditioning circuitry is fairly straight forward. The infrared LED illuminator array (Figure 3.10) is driven by a 0 to 10 volt digital to analog converter (DAC) via a resistive voltage divider network and an NPN bipolar junction transistor emitter follower circuit which serves to boost the available current to a suitable drive level.

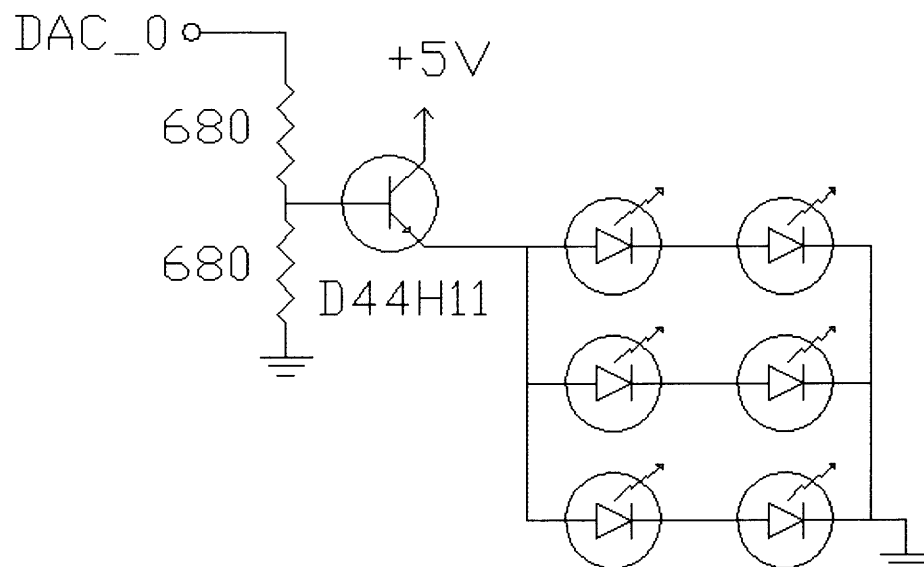


Figure 3.10 IRLED illuminator circuitry.

The decision to control the illuminator via DAC was made to facilitate modulation. Modulating the illumination could serve –when combined with detector filtering- to automatically reject low frequency noise and offset errors introduced by ambient lighting. In testing it was found that noise in subdued ambient lighting was sufficiently negligible and the DAC has since served in a static dimming capacity to calibrate the illuminator level well below that of detector saturation.

The photodetector circuit (Figure 3.11) is equally simple. It consists of a negatively biased photodiode feeding an analog to digital converter (ADC) via a high (10 Megaohm) input impedance (HI-Z) non-inverting amplifier with a gain that may be varied up to approximately 200 using a 200 kiloohm multiturn trimmer potentiometer.

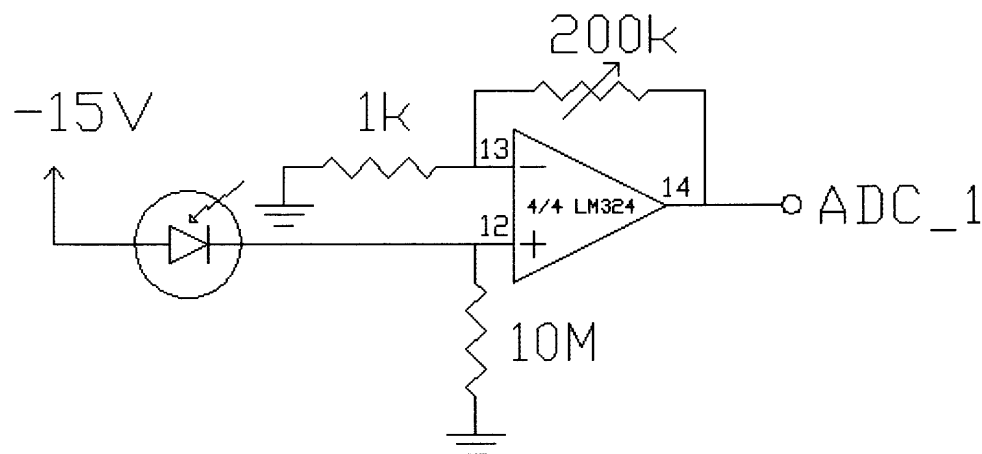


Figure 3.11 Photodetector circuitry.

The force sensing circuit (Figure 3.12) consists of the aforementioned full bridge strain gage based load cell from Figure 3.4, biased with +5 volts, and feeding an ADC via an instrumentation amplifier with a nulling network added to the non-inverting leg of the summing amplifier section. Offset null and gain are adjusted via 20 k Ω multiturn potentiometers.

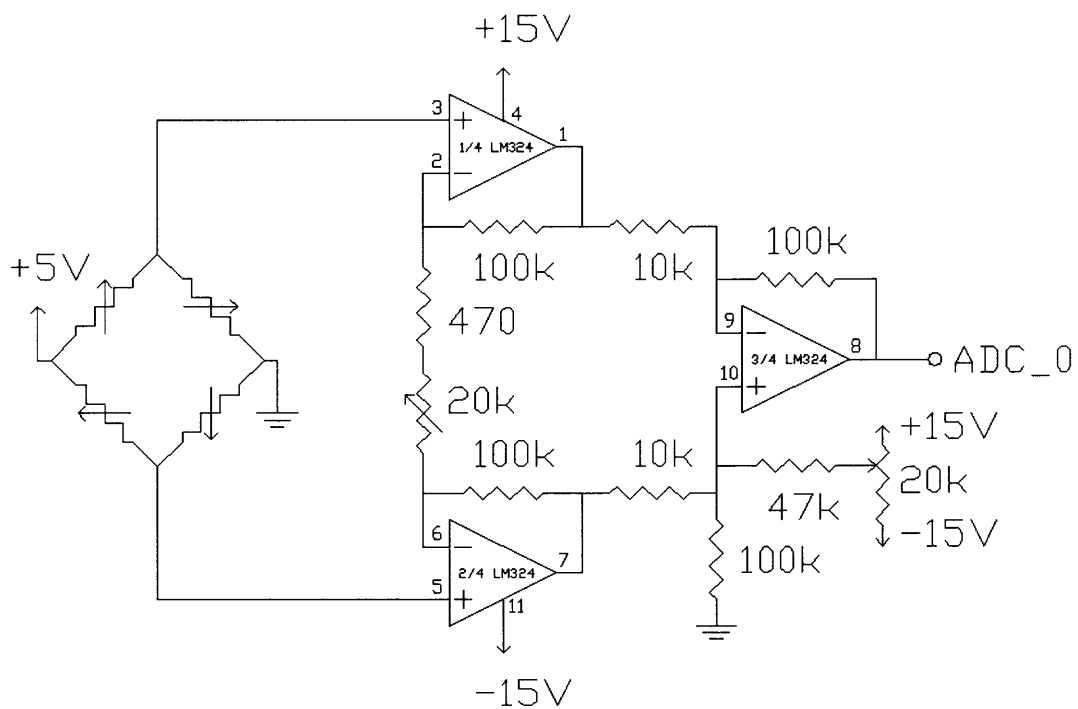


Figure 3.12 Load cell signal conditioning circuitry.

All of the acquisition signal conditioning circuitry (Figure 3.13) was assembled on a small thru-plated hot leveled tin perforated breadboard with pad to pad Teflon insulated jumper wiring designed to sit in the prototype's sensing head to minimize HI-Z transmission length. All but the 10M Ω fixed resistors are SMDs mounted on the back.

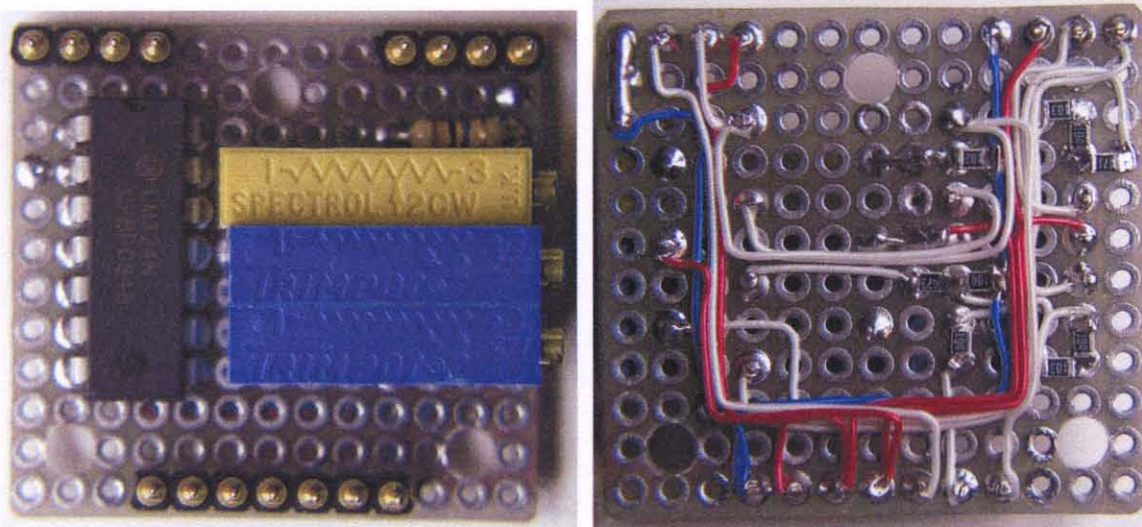


Figure 3.13 Signal conditioning circuitry from sensing head corresponding to schematic diagrams in Figures 3.11 and 3.12. Potentiometers from top to bottom are photodiode gain, loadcell offset and loadcell gain.

3.3.6 Sensing Head Assembly

The completed sensing head (Figure 3.14) is assembled in a tapered pocket machined acetal (Delrin) polymer block. The circuit board, linear rail and one end of the load cell are attached to the base of the milled pocket. The other end of the load cell and the probe tip are attached to the linear rail carriage via a hollow cube shaped aluminum bracket.

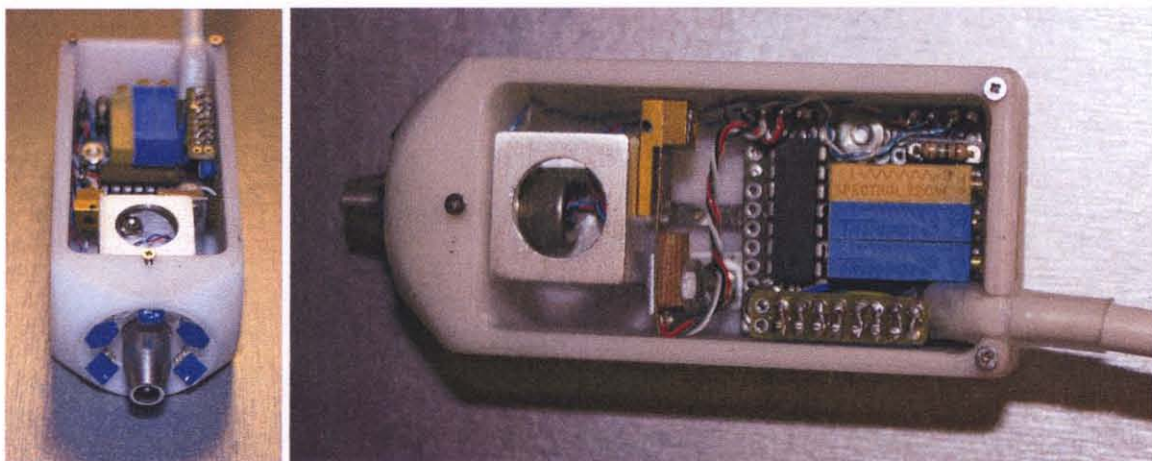


Figure 3.14 Sensing head showing photodetecting probe tip and six element IR illuminator (left) and signal conditioning circuitry, cube shaped angle bracket riding on recirculating ball slide, loadcell assembly and tether cable connector (right).

The sensing head is tethered to a polycarbonate enclosure (Figure 3.15) containing power conditioning and isolation circuitry, the illuminator's driver transistor and BNC terminated pigtailed which connect to the data acquisition card's (DAQ's) ADCs and DAC ports. A second level of isolation is provided by a medically isolated Ault brand MW117 switching power supply. The complete system can be seen in Figure 3.16.

3.3.7 Data Acquisition System

At the current stage of concept development, in lieu of interfacing to, and programming a microcontroller IC, it was decided that data acquisition using a personal computer and DAQ would be more illustrative. The Daqboard2000 DAQ and associated DBK206 breakout board manufactured by IOTECH were selected and configured for use with National Instruments' Labview virtual instrument (VI) development environment.

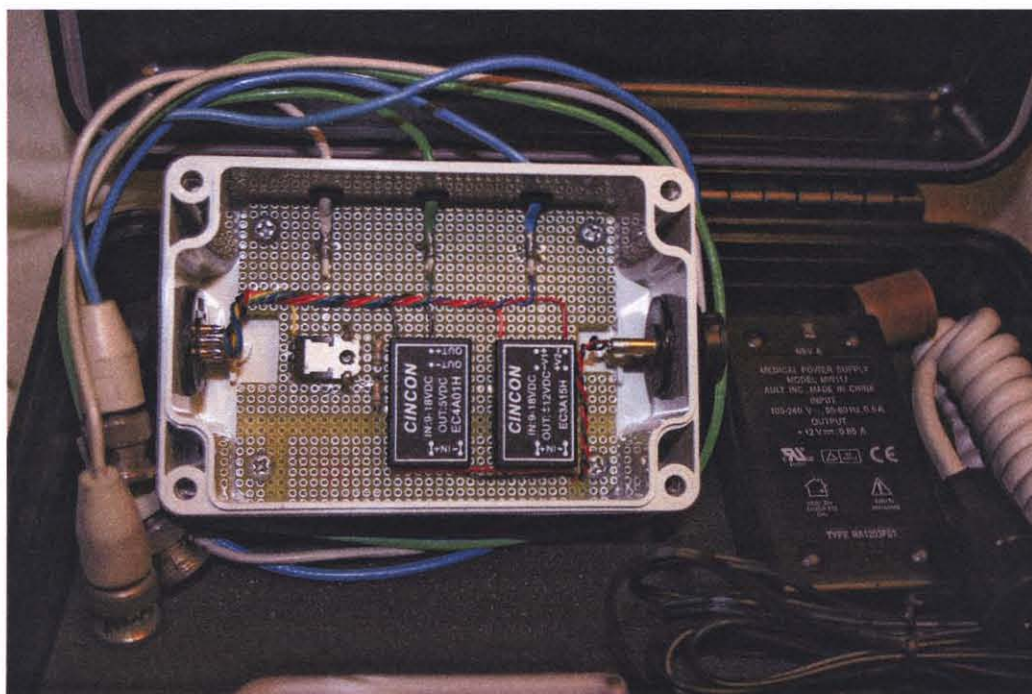


Figure 3.15 Power conditioning and signal junction circuitry showing (from left to right) 3 BNC connectors (2 ADC and 1 DAC) for PC DAQ card, quick disconnect for sensing head's tether cable, power transistor for IR LED drive, isolated DC to DC power converter modules, external power supply quick disconnect and supply.

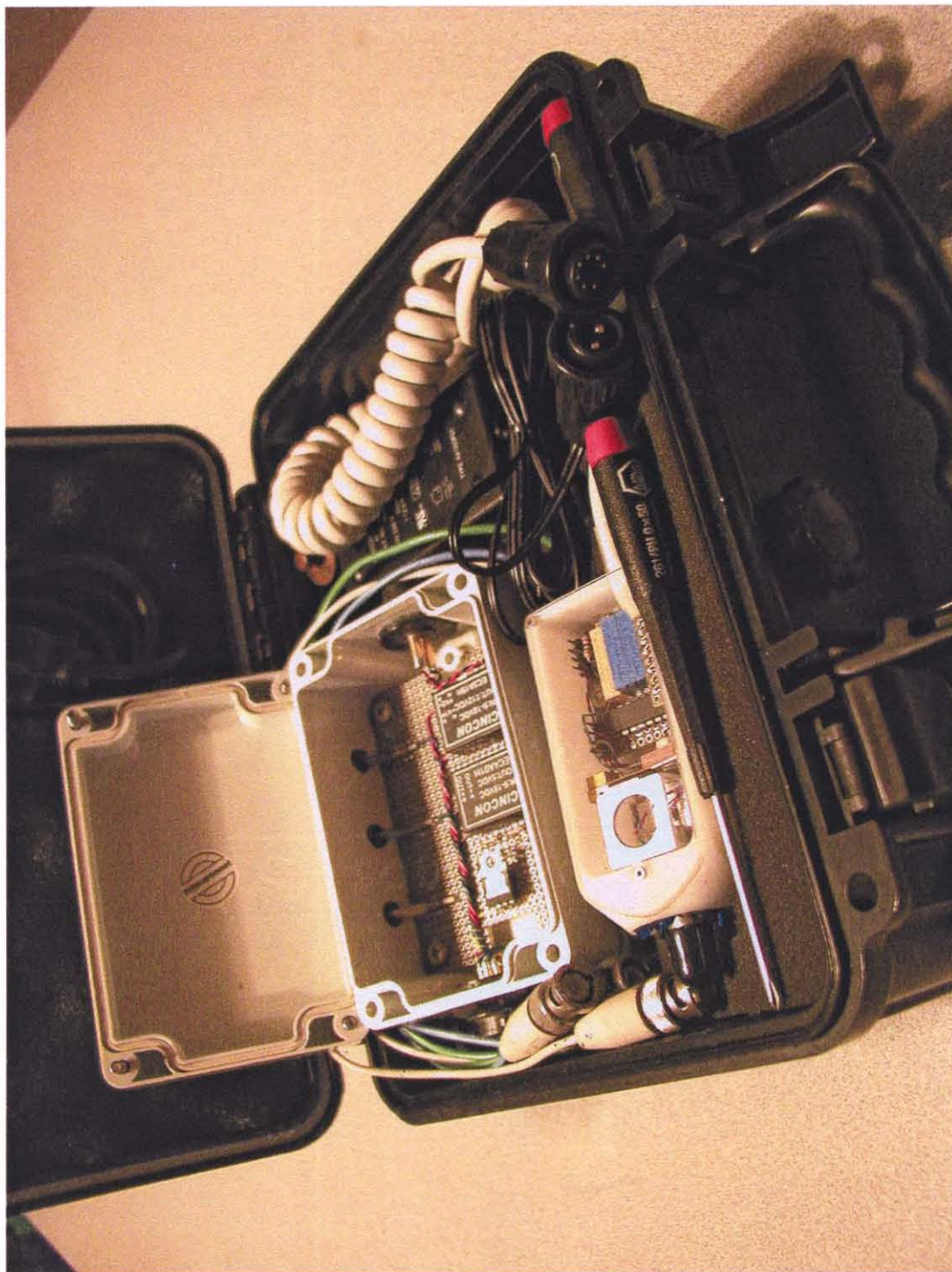


Figure 3.16 Complete system.

Two VIs (Figure 3.17 and detailed in the appendix) were implemented to control the DAC and coordinate the acquisition from the two ADCs. The ADCs are continuously sampled at a repetition rate of 1000 Hertz until the applied force reaches 95 grams at which point the data buffer is transferred to an Excel file for later analysis.

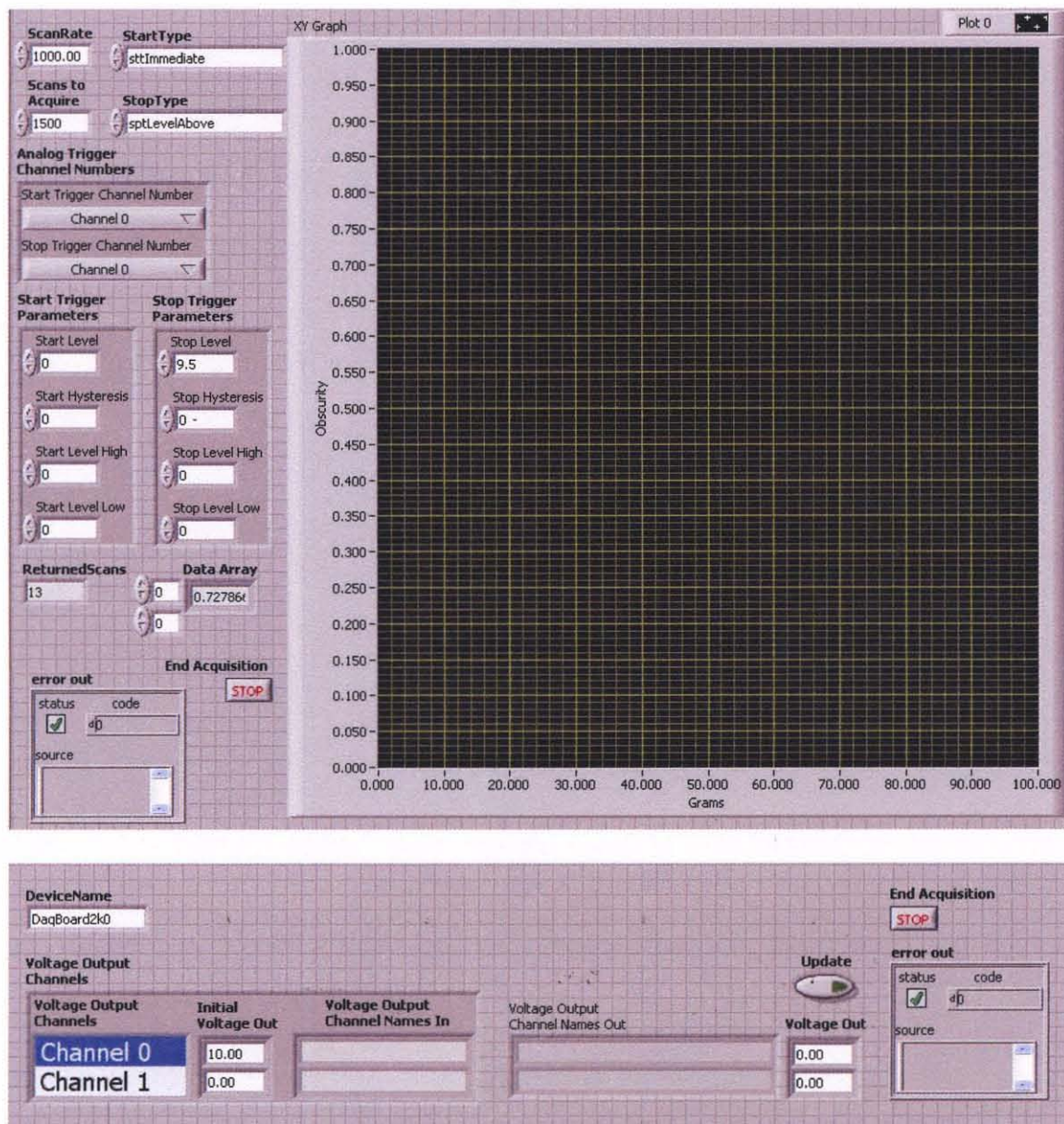


Figure 3.17 Virtual instruments.

CHAPTER 4

RESULTS

4.1 Clinical Trial

Three subjects participated in a clinical trial which involved –in order of execution- the following procedures:

- Goldman applanation tonometry was performed on both eyes. [14]
- Sampling with the prototype device was performed on both eyes.
- Subjects laid supine for approximately 10 minutes. [14] [16]
- Goldman applanation tonometry was again performed on both eyes.
- Sampling with the prototype device was again performed on both eyes.

4.1.1 Goldman Applanation Tonometry

Goldman applanation tonometry was performed using the standard protocol -as briefly described herein in section 1.2.3 and Figure 1.4- by an ophthalmic clinician at the University of Medicine and Dentistry of New Jersey at the Newark, New Jersey campus in accordance with IRB approval.

4.1.2 Prototype Device Sampling

The prototype device's DAQ was configured to begin sampling once the output of the photodetector circuit reached below a preset (negative) threshold voltage which is indicative of illuminator reflection and thus of the probe tip approaching the palpebra. Likewise, the DAQ was configured to stop sampling and save the data to an Excel compatible comma delimited file once the load cell circuit's output voltage reached a

preset threshold indicating that sufficient force was applied. Subjects were asked to conduct the test on themselves under our team's supervision with the test consisting of closing each eye's palpebra and touching it with the probe tip four or five times.

Purely for the reader's amusement, Figure 4.1 illustrates the results of three typical tests in the form of three stereograms. Those readers capable of converging upon the stereo pairs –crossing their eyes slightly as they hold the page straight and at arms length- can view these images in 3D.

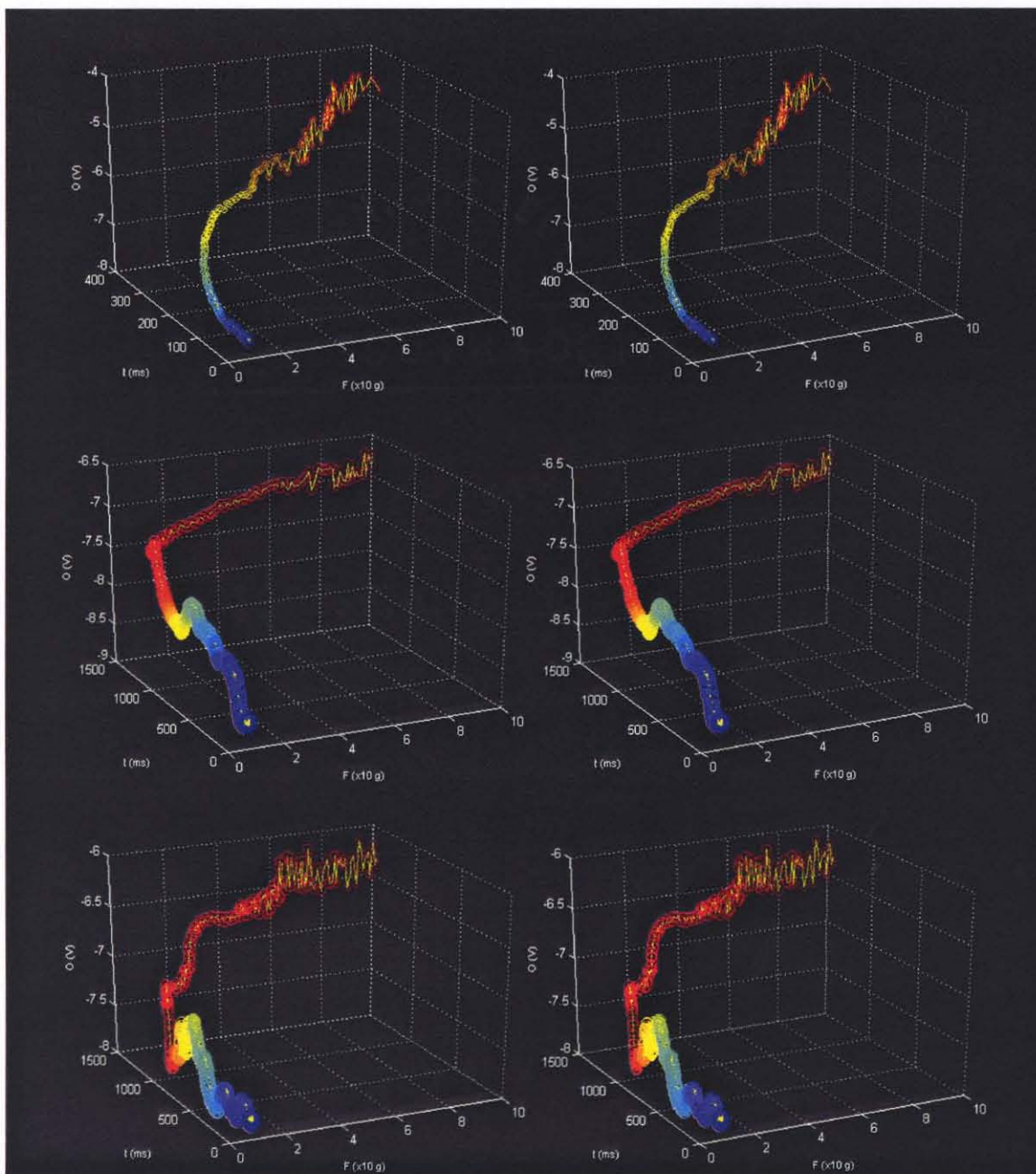


Figure 4.1 Stereoscopic images of three typical time sample series.

Data from tests which timed-out prior to completion were discarded and the tests repeated after the subjects were instructed to proceed in a faster more fluid motion.

It can be seen that the curves are ill-behaved in the time domain but this variable can be eliminated as illustrated by a 2D scatter plot (Figure 4.2).

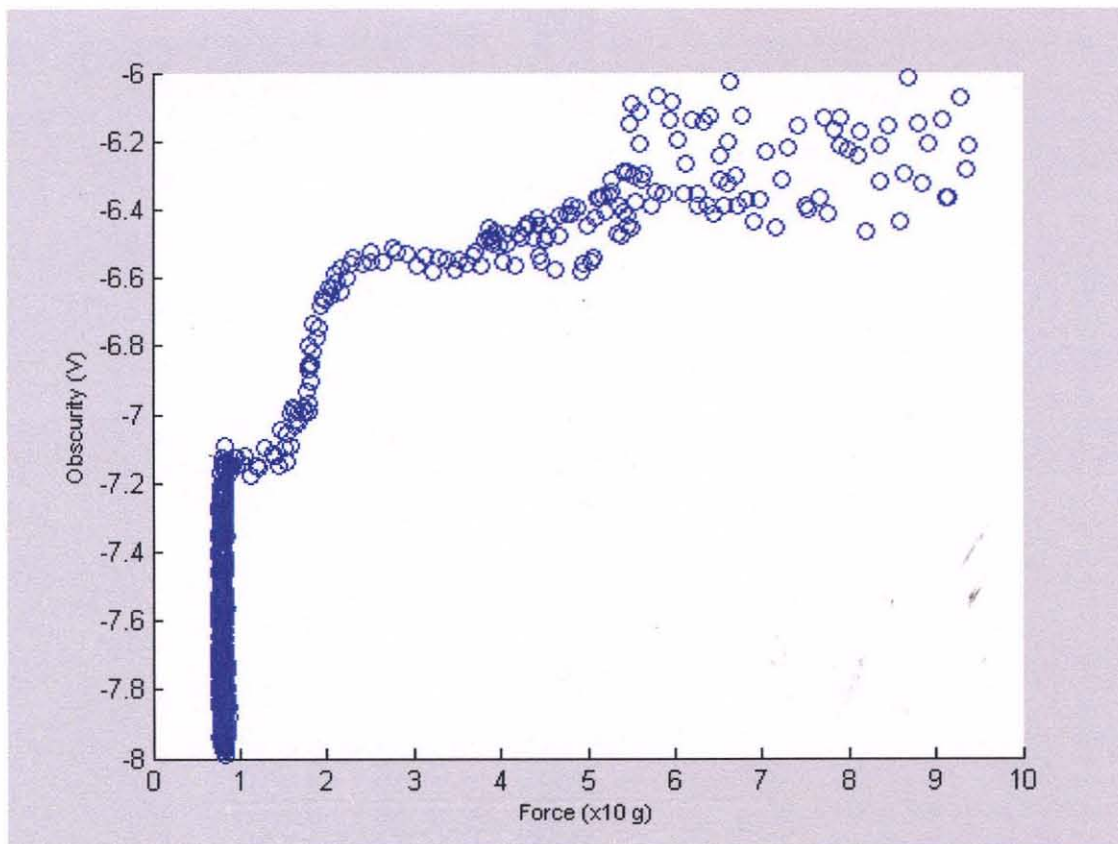


Figure 4.2 Scatter plot of typical test data. The vertical region on the left corresponds to obscuration of the probe tip just prior to contact with the palpebra.

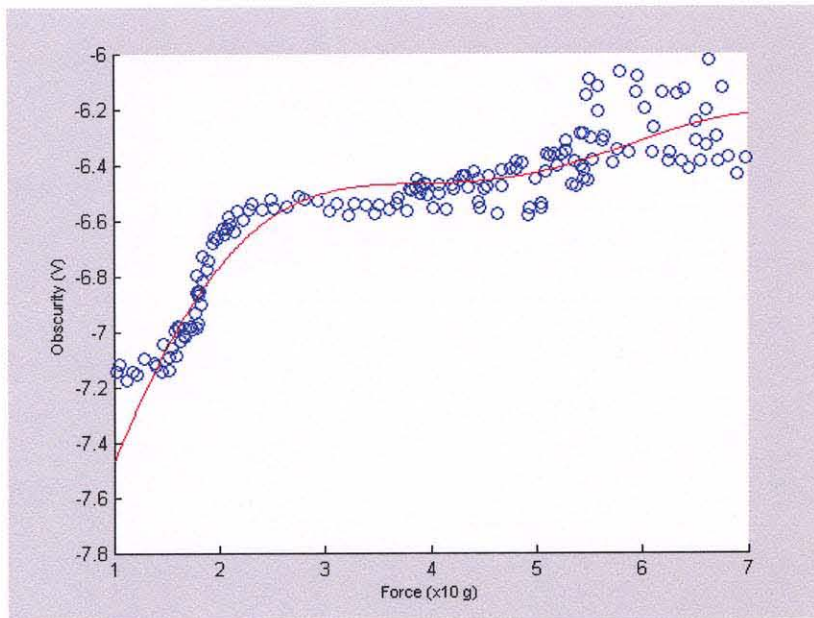


Figure 4.3 6th order polynomial fit.

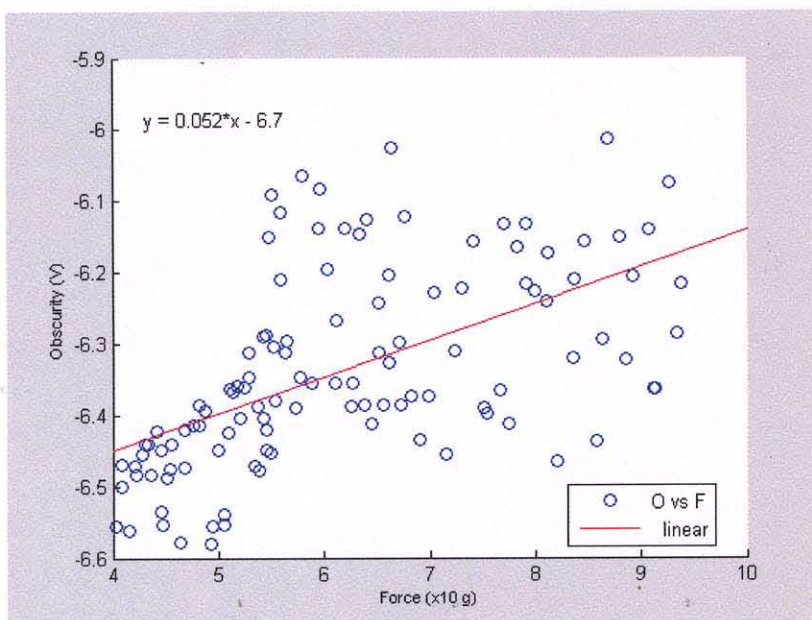


Figure 4.4 Linear fit.

Fitting a 6th order polynomial as drawn in red in Figure 4.3 illustrates the expected response consisting of palpebral compression (up to around 20g), corneal pre-compression (20g to 35g), and corneal compression (35g to 60g).

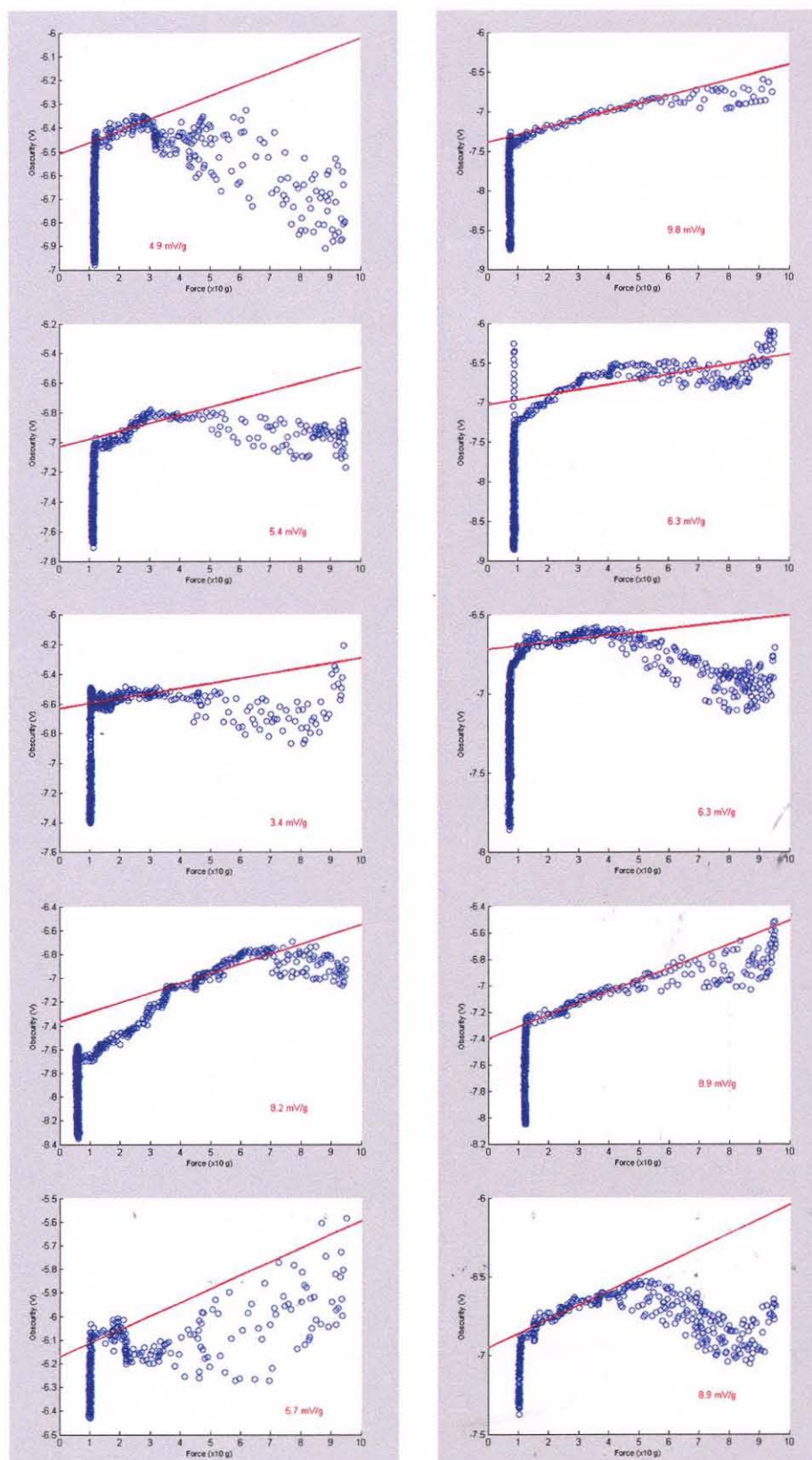


Figure 4.5 Subject #1 pre-supine averages of 5 trials are: L=5.5mV/g, R=8.0mV/g.

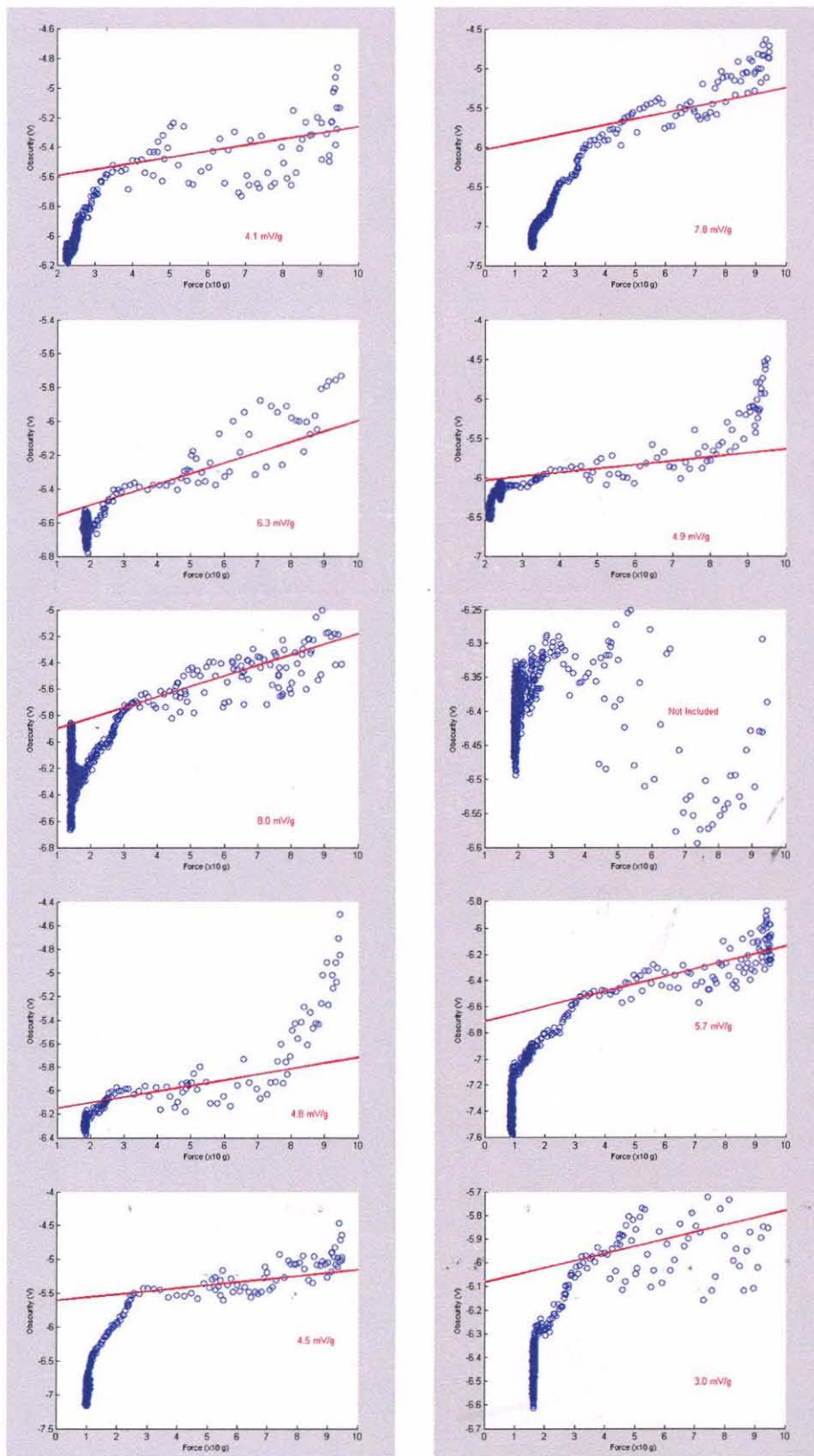


Figure 4.6 Subject #2 pre-supine average compliances: L=5.5mV/g, R=5.4mV/g.

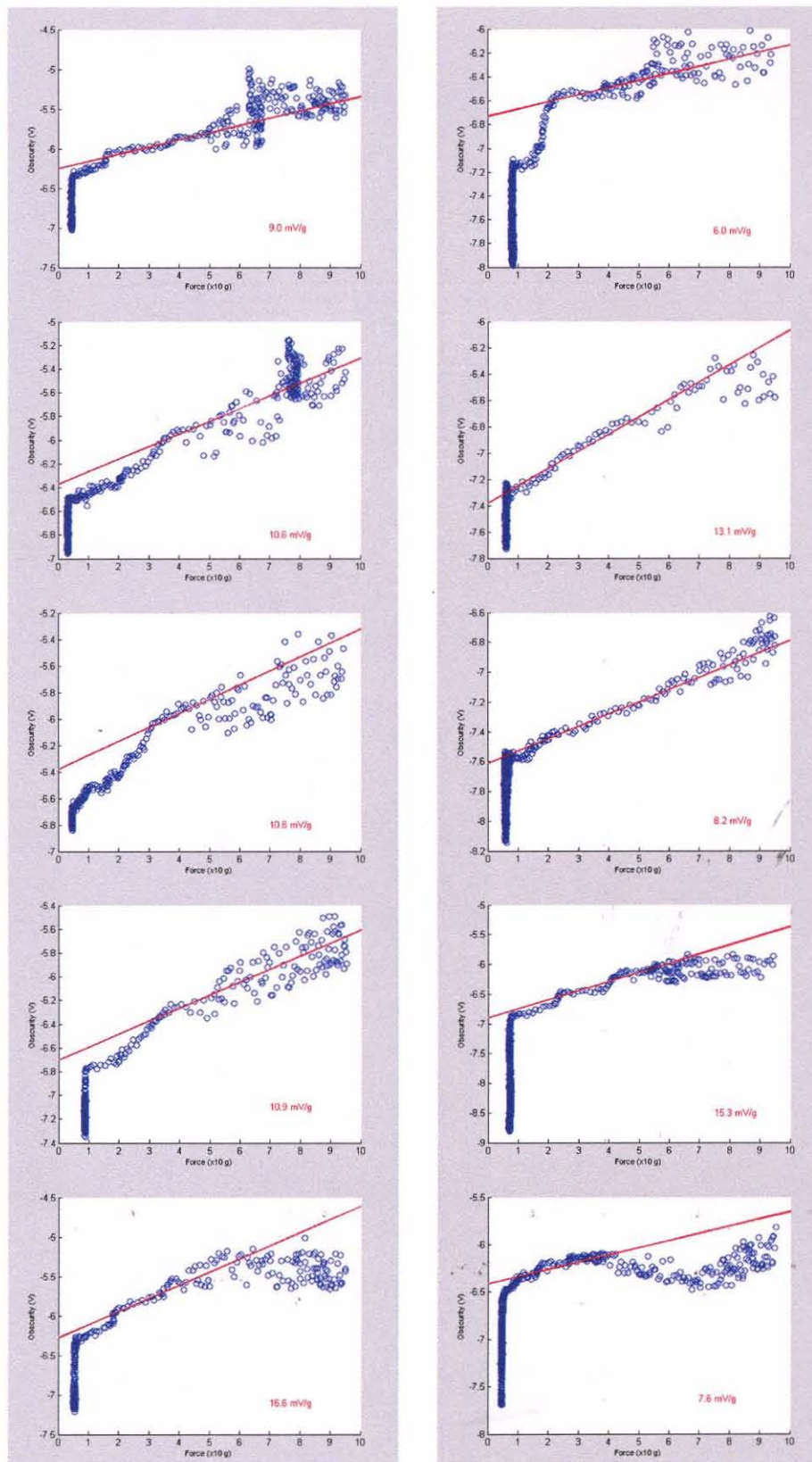


Figure 4.7 Subject #3 pre-supine average compliances: L=12mV/g, R=10mV/g.

A linear interpolation (Figure 4.4) of the latter region –who’s slope shall be called corneal compliance in mV/g- was conducted (Figures 4.5 – 4.10) -averaging corneal compliances of each eye’s tests- yielding the twelve compliance results in Table 4.1 (one for each eye of the three subjects both pre and post the supination period). The reciprocal of the compliance –which shall be called corneal rigidity- is then calculated as

$\frac{1000}{\text{Compliance}}$ as it better compares to the Goldman Reference test.

Table 4.1 Experimental Results

Subject	Compliance mV/g	Rigidity g/V	Goldman Reference mmHg
#1 Pre-sup., Left eye	5.5	182	19
#1 Pre-sup. Right eye	8.0	125	17
#2 Pre-sup. Left eye	5.5	182	20
#2 Pre-sup. Right eye	5.4	185	20
#3 Pre-sup. Left eye	12	83	14
#3 Pre-sup. Right eye	10	100	15
#1 Post-sup. Left eye	5.2	192	20
#1 Post-sup. Right eye	7.8	128	17
#2 Post-sup. Left eye	7.0	143	18
#2 Post-sup. Right eye	4.8	208	21
#3 Post-sup. Left eye	11	91	14
#3 Post-sup. Right eye	14	71	12

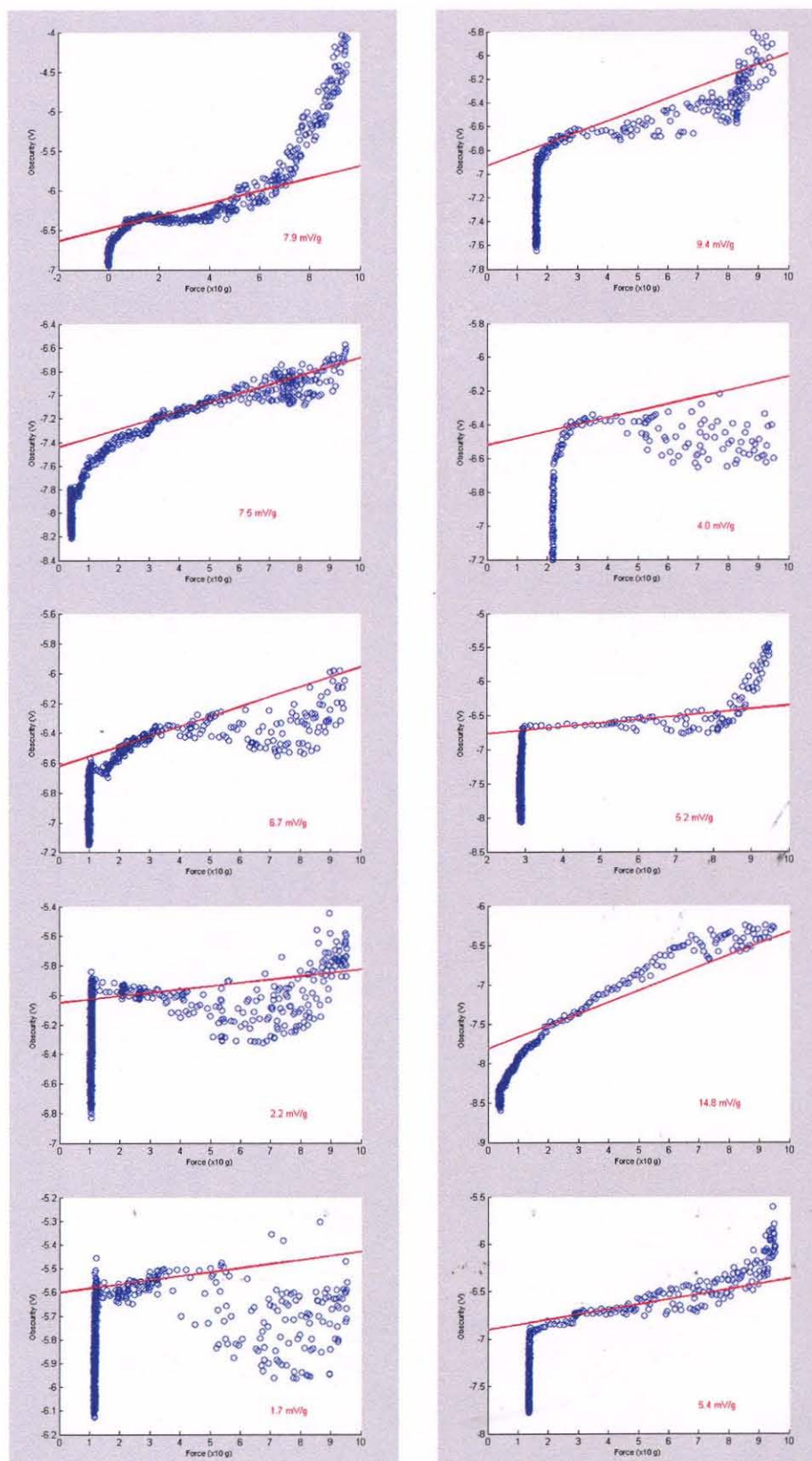


Figure 4.8 Subject #1 post-sup. average compliances: L=5.2mV/g, R=7.8mV/g.

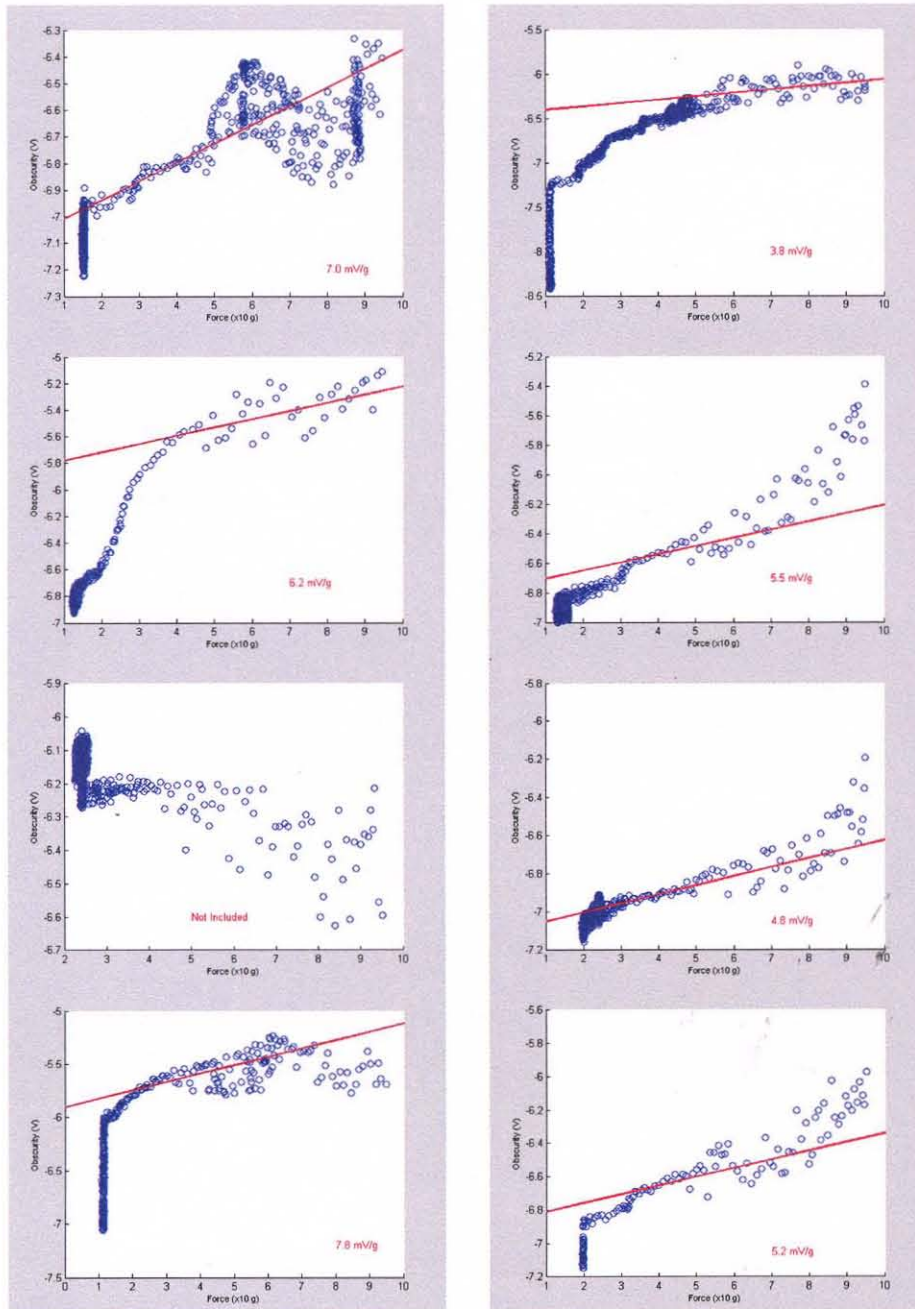


Figure 4.9 Subject #2 post-sup. average compliances: L=7.0mV/g, R=4.8mV/g.

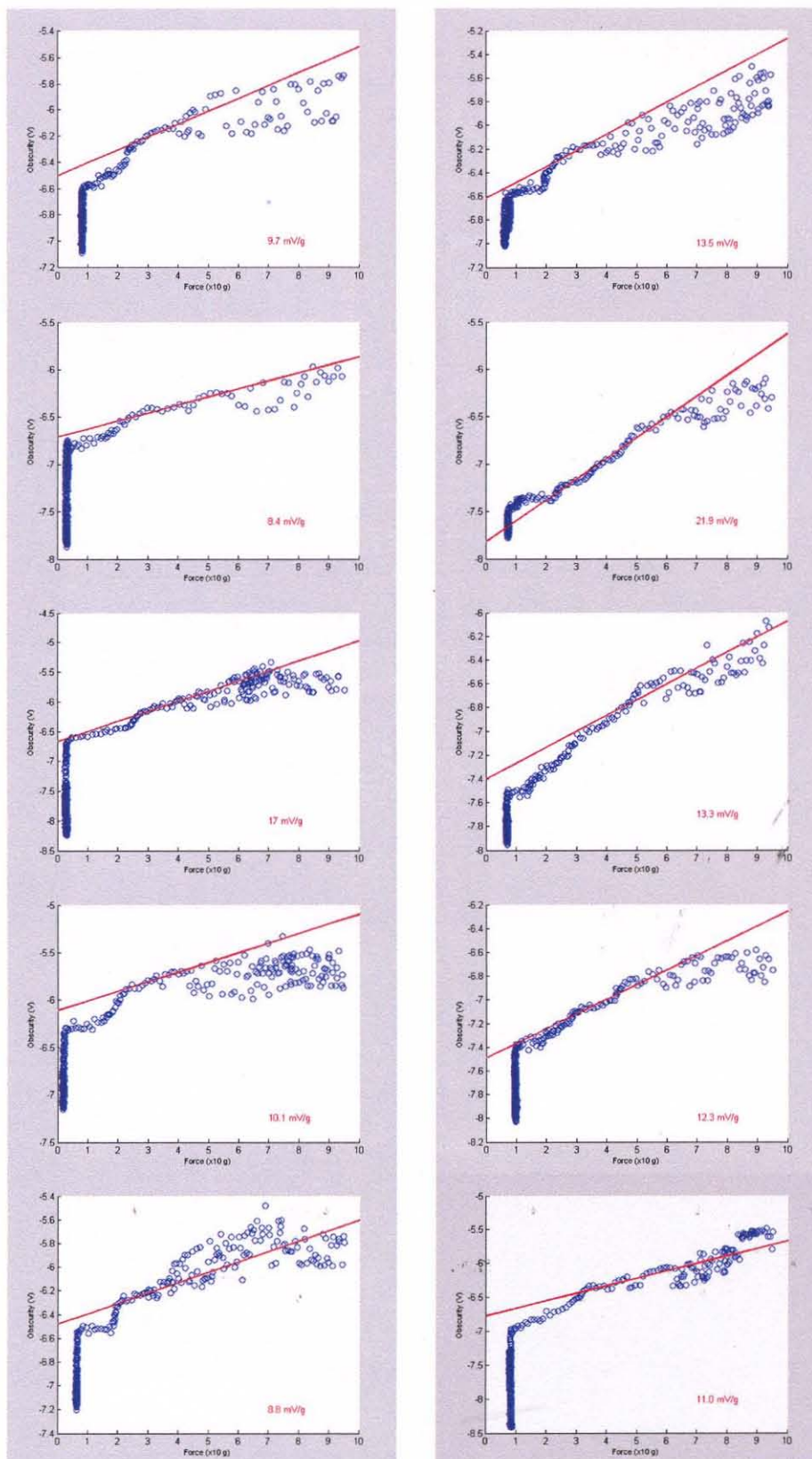


Figure 4.10 Subject #3 post-sup. average compliances: L=11mV/g, R=14mV/g.

CHAPTER 5

CONCLUSION

5.1 Comparison

The experimental results in Table 4.1 are compared in Figure 5.1 by plotting the rigidity values measured using the prototype device with respect to the reference standard pressure measured by Goldman applanation tonometry .

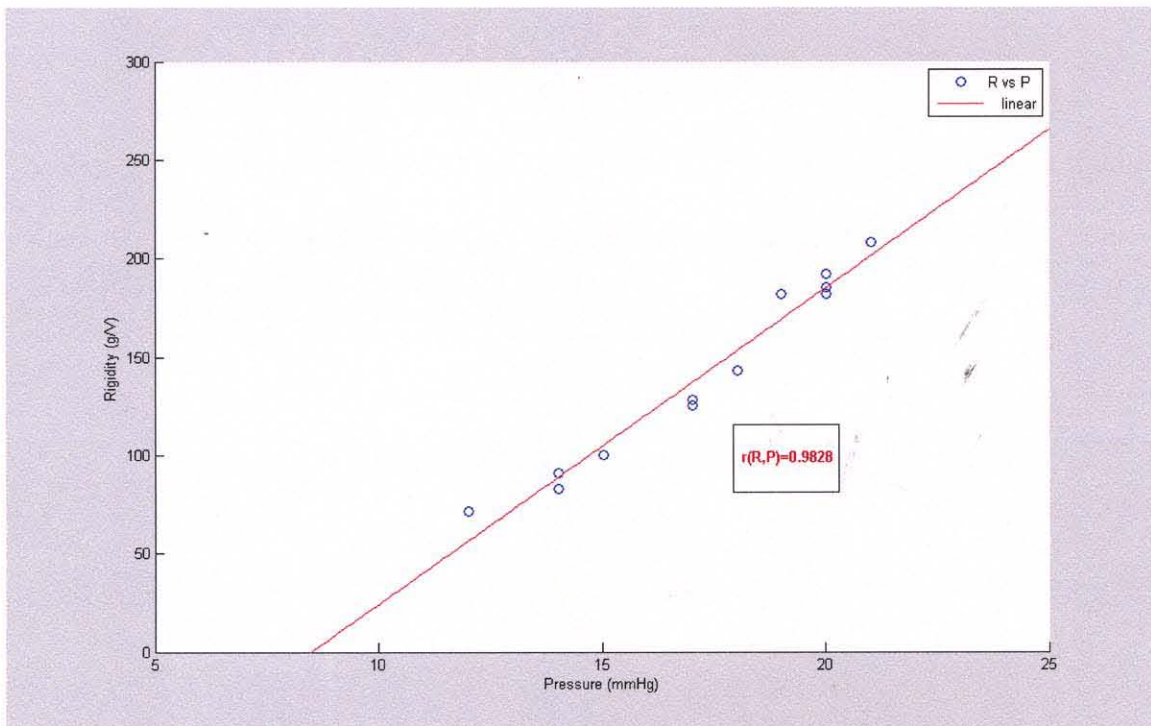


Figure 5.1 Correlation coefficient for prototype device versus Goldman applanation.

Considering that no subject specific calibration was performed on the prototype device, the computation of a Pearson correlation coefficient of 0.9828 is by far more impressive than had ever been expected.

It is clear that this design concept is sound and merits further development.

5.2 Future Work

Here are some thoughts on future development for production economization, miniaturization and improving reliability and ease of use.

5.2.1 Illuminator Design

Redesign of the illuminator is likely to be one of the most significant size reduction factors in migrating from conceptual prototype to production design. One space saving idea involves illumination delivery the via optical fibers embedded into and protruding from the periphery of the probe tip.

5.2.2 Linear Guide Mechanism

One of the costliest components incorporated into the prototype is the dual recirculating linear ball slide. The slide could be replaced by a less costly set of six microminiature ball bearings arranged radially in two sets of three around a hexagonal sliding center shaft.

5.2.3 Intuitive Azimuthal Orientation

Off axis application of the device seems to be one of the leading causes of erroneous readings. One idea for providing intuitive orientation feedback would involve replacing the photodiode with a transparent optical component of similar shape which would incorporate a ring of photodetectors as well as a thinly collimated visible light source delivered via an opaque tube at the component's center. By keeping the light in view while performing the tests, a subject would be assured of keeping the probe normal to the surface of the eye.

APPENDIX

LABVIEW DATA ACQUISITION VIRTUAL INSTRUMENT BLOCK DIAGRAMS

Figure A.1 depicts the overview of the Labview virtual instruments (VIs) block diagram used for data acquisition in the clinical trials.

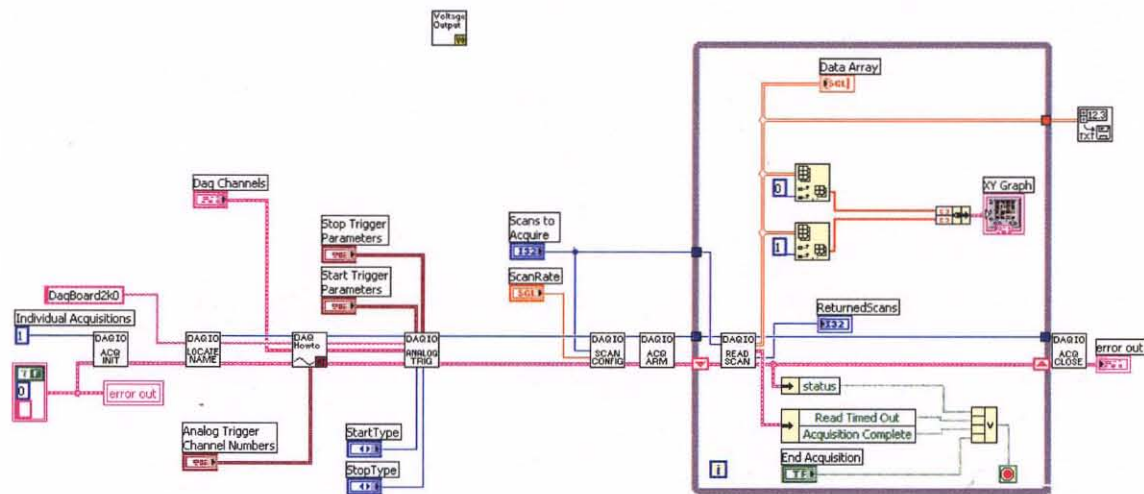


Figure A.1 Labview VIs block diagram overview.

The data acquisition system which was used (an IOtech Daqboard 2000 and its associated DBK206 screw terminal breakout card) allows for autonomous buffered block sampling. The first of the initialization VIs (Figure A.2) is used to set the number of autonomous samples to 1 and to initialize an error flag to 'false'.

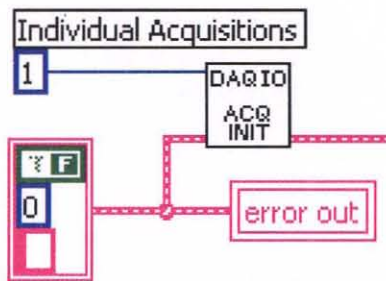


Figure A.2 Acquisition initialization VI.

The next block in the initialization path (Figure A.3) appends the identification label 'DaqBoard2k0' which points to the specific DAQ board to be used.

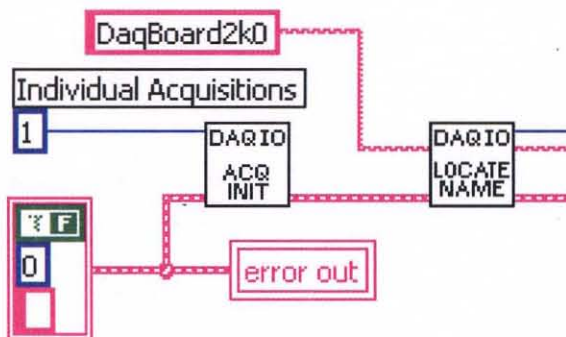


Figure A.3 Board enumeration.

The next two VIs in the chain (Figures A.4 and A.5) incorporate the list of channels to acquire from (channels 0 for force and 1 for illumination in this case) as well as which channels should be considered –and how- in start and stop triggering. In this case, acquisition is set to start automatically (no start trigger) and to stop if the loadcell registers in excess of 95 grams.

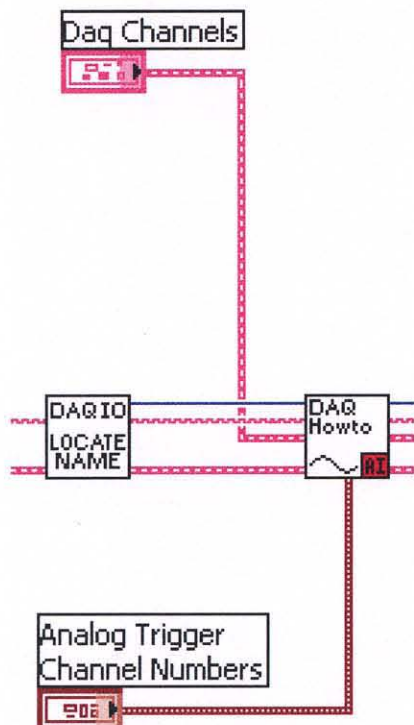


Figure A.4 Channel and trigger enumeration.

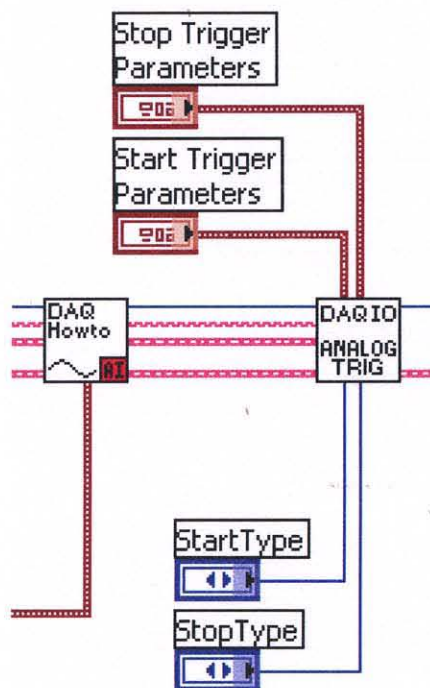


Figure A.5 Trigger parameters.

The last two VIs (Figure A.6) that are included prior to the execution thread entering the sampling 'while loop' set the number of single sample scan iterations (1500 here) and the delay interval between them (1ms here) and then arm the acquisition subsystem. This provides 1.5 seconds in which to complete each trial. Sampling is automatically restarted until the force threshold is reached.

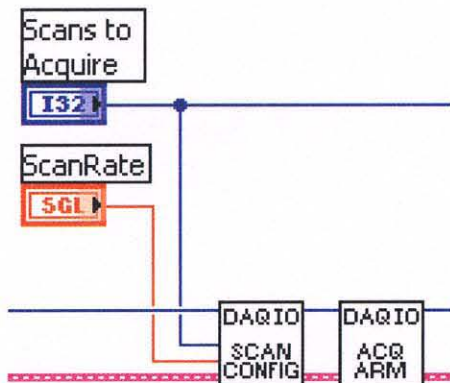


Figure A.6 Scans.

Within the 'while loop' (Figure A.7), a sample from each channel is acquired every millisecond and stored in a data array. If an error occurs or if the force threshold is reached, the data array is output to a prenamed Excel compatible text file. If the acquisition 'times out', the while loop simply restarts.

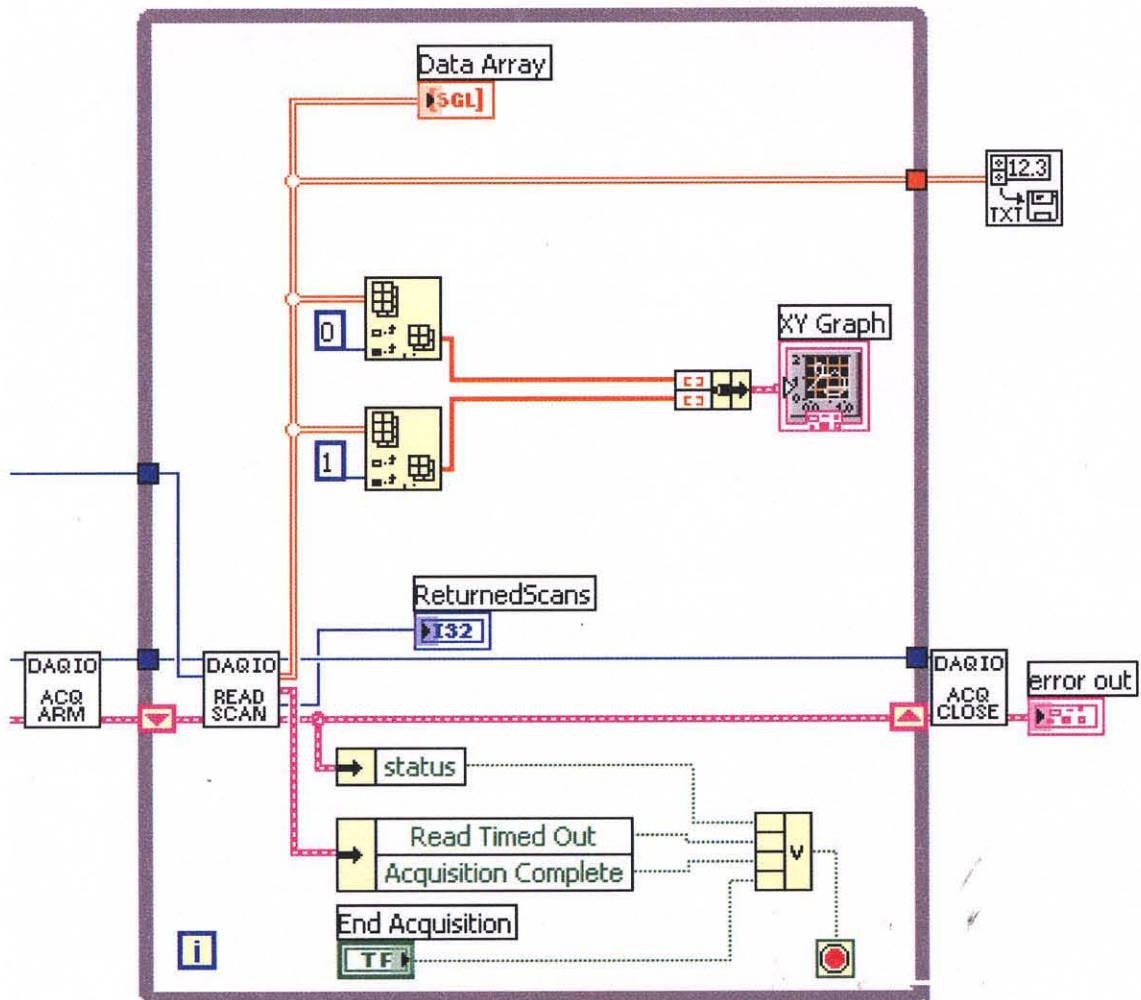


Figure A.7 While loop.

REFERENCES

1. A. Asrani, R. C. Zeimer, J. D. Gieser, S. Vitale, and K. Lindenmuth, "Large Diurnal Fluctuations in Intraocular Pressure are an Independent Risk Factor in Patients with Glaucoma," *J. Glaucoma*, Apr;9(2):134-42., 2000.
2. R. C. Zeimer, J. T. Wilensky, and D. K. Gieser, "Presence and Rapid Decline of Early Morning Intraocular Pressure Peaks in Glaucoma Patients," *Ophthalmology*, May;97(5):547-50, 1990.
3. T. L. Alvarez, S. A. Gollance, G. A. Thomas, R. J. Greene, P. M. Marchetto, E. J. Moore, T. Realini, J. M. Liebmann, R. Ritch, P. Lama, and R. D. Fechtner, "The Proview Phosphene Tonometer Fails to Measure Ocular Pressure Accurately in Clinical Practice," *Ophthalmology*, 111(6), pp. 1077-1085, 2004.
4. G. Wyszecki, W. S. Stiles, "Concepts and Methods, Quantitative Data and Formulae," *Color Science*, 1982.
5. R. Masland, "The Functional Architecture of the Retina," *Sci. Amer.*, pp. 102-111, 1986.
6. J. Jackson, L. W. Carr, B. M. Fisch, V. E. Malinovsky, D. K. Talley, "Optometric Clinical Practice Guideline Care of the Patient with Primary Angle Closure Glaucoma," *American Optometric Association Reference Guide for Clinicians*, 1994.
7. J. de Kock, L. Tarassenko, C. Glynn, and A. Hill "Reflectant Pulse Oximetry Measurements from the Retinal Fundus," *IEEE Trans Biomed*, 40(8), pp. 817-823, 1993.
8. National Eye Institute, Bethesda, MD, Public Health Service, National Institutes of Health, U.S. Depart of Health Human Services, "Summary and Critique of Available Data on the Prevalence and Economic and Social Costs of Visual Disorders," *US DHHS*, 1976.
9. D. S. Friedman et al., "Prevalence of Open-Angle Glaucoma Among Adults in the United States," 122:532-538, Arch., *Ophthalmology*, 2004.
10. American Academy of Ophthalmology, "Benchmarks for Preferred Practice Patterns," *Summary*, SF, 2001:3.
11. R. S. Mackay, E. Marg, R. Oechsli, "Automatic Tonometer with Exact Theory: Various Biological Applications," 3;131:1669-9, *Science*, Jun, 1960.

12. R. C. Zeimer et al., "Evaluation of a Self-Tonometer for Home Use," 101:1791-3, *Arch., Ophthalmology*, 1983.
13. B. B. Fresco, "A New Tonometer – The Pressure Phosphene Tonometer: Clinical Comparison with Goldman Tonometry," 105:2123-6, *Ophthalmology*, 1998.
14. J. H. K. Liu, A. J. Sit, R. N. Weinreb, "Variations of 24-Hour Intraocular Pressure in Healthy Individuals – Right Eye Versus Left Eye," Oct;10;112:1670-4, *Ophthalmology*, 2005.
15. J. Ma, D. Xu, "A Miniaturized Applanation Tonometer," Aug;8;46, *IEEE Transactions on Biomedical Engineering*, 1999.
16. Personal communication with R. D. Fectner of [3] in 9/2007.